

# Continuous-discrete smoothing of diffusions

Marcin Mider<sup>1</sup>, Moritz Schauer<sup>2</sup> and Frank van der Meulen<sup>3</sup>

<sup>1</sup>*Max Planck Institute for Mathematics in the Sciences, 04103 Leipzig, Germany, e-mail: marcin.mider@mis.mpg.de*

<sup>2</sup>*Department of Mathematical Sciences, Chalmers University of Technology and University of Gothenburg, Chalmers Tvärsgata 3, 41296 Göteborg, Sweden, e-mail: smoritz@chalmers.se*

<sup>3</sup>*Delft Institute of Applied Mathematics (DIAM), Delft University of Technology, Van Mourik Broekmanweg 6, 2628 XE Delft, The Netherlands, e-mail: f.h.vandermeulen@tudelft.nl*

**Abstract:** Suppose  $X$  is a multivariate diffusion process that is observed discretely in time. At each observation time, a linear transformation of the state of the process is observed with noise. The smoothing problem consists of recovering the path of the process, consistent with the observations. We derive a novel Markov Chain Monte Carlo algorithm to sample from the exact smoothing distribution. The resulting algorithm is called the *Backward Filtering Forward Guiding (BFFG) algorithm*. We extend the algorithm to include parameter estimation. The proposed method relies on guided proposals introduced in [Schauer et al. \(2017\)](#). We illustrate its efficiency in a number of challenging problems.

**Keywords:** *chemical reaction network, data assimilation, diffusion bridge, filtering, guided proposal, Lorenz system, Markov Chain Monte Carlo, partial observations, stochastic heat equation on a graph.*

**MSC 2010 subject classifications:** Primary 60J60, 65C05; secondary 62F15.

## 1. Introduction

Suppose  $X$  is a diffusion process with dynamics governed by the stochastic differential equation (SDE)

$$dX_t = b(t, X_t) dt + \sigma(t, X_t) dW_t \quad (1.1)$$

with prescribed initial distribution  $X_{t_0} \sim \pi(x_{t_0})$ . Here  $b: \mathbb{R}_+ \times \mathbb{R}^d \rightarrow \mathbb{R}^d$  and  $\sigma: \mathbb{R}_+ \times \mathbb{R}^d \rightarrow \mathbb{R}^{d \times d}$  are the drift and dispersion coefficient respectively. The process  $W$  is a vector valued process in  $\mathbb{R}^{d'}$  consisting of independent Brownian motions. It is assumed that the required conditions for existence of a strong solution are satisfied (cf. [Karatzas and Shreve \(1991\)](#)). We assume observation times  $0 = t_0 < t_1 < \dots < t_n$  and observations

$$V_i = L_i X_{t_i} + \eta_i, \quad i = 0, \dots, n, \quad (1.2)$$

where  $L_i$  is a  $m_i \times d$ -matrix and  $\eta_i \sim N_{m_i}(0, \Sigma_i)$  are independent random vectors, independent of the diffusion process  $X$ . Let  $D = \{V_i, i = 0, \dots, n\}$ . The setup includes the practically relevant case that a highly non-linear process  $X$  is only observed at start time 0 and at a final time, say 1, see for instance [Arnaudon et al. \(2020\)](#) for an application in shape analysis.

In this article we address two related problems: *smoothing* and *inference*. For the first one we assume that  $b$ ,  $\sigma$  and  $\{\Sigma_i, i = 0, \dots, n\}$  are known, and aim to reconstruct the path  $\{X_t, t \in [0, t_n]\}$  based on  $D$ , which here is given precise meaning as sampling from the conditional

distribution of  $X$  on  $[0, t_n]$  given  $D$ . Because we are dealing with “continuous dynamics-discrete observations”, this setup is also referred to as continuous-discrete smoothing or hybrid smoothing. This is an interesting problem in its own right that arises naturally, for instance, in applications to data analysis of tracking systems (cf. [Särkkä \(2013\)](#)).

Additionally, it constitutes a central component of Bayesian inference algorithms for discretely observed diffusions. If in (1.1) the coefficients of the diffusion  $X$  or the measurement noise  $\{\eta_i, i = 0, \dots, n\}$  depend on some unknown parameters, inference can be performed by employing a data augmentation algorithm, where one iterates between (i) updating the parameter conditional on the smoothed path and (ii) continuous-discrete smoothing conditional on the value of the parameter (cf. [Roberts and Stramer \(2001\)](#)). The relevance of smoothing and parameter estimation for diffusions is illustrated from the problem reappearing in a wide variety of application fields, see for instance [van Kampen \(1981\)](#), [Arnaudon et al. \(2017\)](#), [Apte et al. \(2007\)](#), [Cuenod et al. \(2011\)](#) and [Wilkinson \(2006\)](#).

### 1.1. Related work

If the full state of the diffusion process is observed at all times  $\{t_i, 0 \leq i \leq n\}$  without noise, i.e. if  $L_i = I$  and  $\eta_i \equiv 0$  for all  $i$ , then the smoothing problem reduces to the sampling of  $n$  independent diffusion bridges. This problem has attracted considerable attention over the past two decades, see for instance [Eraker \(2001\)](#), [Elerian et al. \(2001\)](#), [Durham and Gallant \(2002\)](#), [Clark \(1990\)](#), [Bladt et al. \(2016\)](#), [Beskos et al. \(2008\)](#), [Hairer et al. \(2009\)](#), [Bayer and Schoenmakers \(2013\)](#), [Lin et al. \(2010\)](#), [Beskos et al. \(2006\)](#), [Delyon and Hu \(2006\)](#), [Lindström \(2012\)](#), [Schauer et al. \(2017\)](#), [Whitaker et al. \(2017\)](#) and [Bierkens et al. \(2019\)](#). In the general case however, the connecting bridges cannot be sampled independently between adjacent observation times. In fact, at time  $t \in (t_{i-1}, t_i)$  the process  $X$ , conditioned on  $D$ , depends on all future conditionings  $V_i, \dots, V_n$ . To resolve this problem, subsequent simulation of bridges on overlapping intervals has been proposed by [Golightly and Wilkinson \(2008\)](#), [Fuchs \(2013\)](#) and [van der Meulen and Schauer \(2017b\)](#).

[Särkkä and Sottinen \(2008\)](#) considered *filtering* (instead of smoothing) of diffusions under the assumption that the dispersion coefficient is only allowed to depend on time. If the diffusion can be transformed to unit diffusion coefficient, then filtering can also be accomplished using the exact algorithm for simulation of diffusions, as introduced by [Beskos and Roberts \(2005\)](#). This algorithm forms the basis for the methods presented in [Fearnhead et al. \(2008\)](#) and [Olsson and Ströjby \(2011\)](#). Various solutions to the filtering and smoothing problem are further discussed in [Särkkä and Sarmavuori \(2013\)](#). Key to the proposed algorithms therein is the assumption that the distribution of  $X_t$ , conditional on the data  $D$  can be approximated by the normal distribution.

Recently, [Graham et al. \(2019\)](#) considered the same problem as considered here using sampler based on constrained Hamiltonian dynamics. The basic idea is to consider a realisation of SDE-solution as a forward map of Wiener-innovations which are constrained by the observations. Our approach is rather different and fully exploits the structure of the SDE model which yields forward simulation that automatically ensures the observations are taken into account.

## 1.2. Approach

Conceptually, we follow closely the literature on *guided proposals*. We explain the main idea here, postponing details to Section 2. To this end, assume  $X$  admits smooth transition densities  $p$ , i.e. for  $s < \tau$ ,  $P^{(s,x)}(X_\tau \in dy) = p(s, x; \tau, y) dy$ . For  $t \in (t_{i-1}, t_i)$ , the process  $X$ , conditioned on  $V_i, \dots, V_n$  and  $X_{t_{i-1}} = x_{t_{i-1}}$  satisfies the SDE

$$dX_t^* = b(t, X_t^*) dt + a(t, X_t^*) r(t, X_t^*) dt + \sigma(t, X_t^*) dW_t, \quad X_{t_{i-1}}^* = x_{t_{i-1}},$$

with  $a(t, x) = \sigma(t, x)\sigma(t, x)'$ ,  $r(t, x) = \nabla_x \log \rho(t, x)$  (considered as a column vector) and  $\rho$  defined by

$$\rho(t, x) = \int p(t, x; t_i, \xi_i) q_n(v_n - L_n \xi_n) \prod_{j=i}^{n-1} p(t_j, \xi_j; t_{j+1}, \xi_{j+1}) q_j(v_j - L_j \xi_j) d\xi_i \cdots d\xi_n. \quad (1.3)$$

Here,  $q_j$  denotes the density of the  $N(0, \Sigma_j)$  distribution. This expression was derived in [Marchand \(2012\)](#) (Theorem 2.3.4) in case  $\Sigma_j \equiv 0$  for all  $j$  and is derived here, in Appendix A, using Doob's  $h$ -transform. As  $p$  is only known in closed form in very specific instances,  $\rho$  is intractable and hence it is not possible to sample  $X^*$  directly using this expression. The key idea in [Schauer et al. \(2017\)](#), which addressed the simpler problem of diffusion bridge simulation, is to replace the unknown transition density  $p$  by a tractable transition density  $\tilde{p}$  of another auxiliary diffusion process  $\tilde{X}$ . The process  $X^\circ$  is introduced, defined as a solution to the SDE

$$dX_t^\circ = b(t, X_t^\circ) dt + a(t, X_t^\circ) \tilde{r}(t, X_t^\circ) dt + \sigma(t, X_t^\circ) dW_t, \quad X_{t_{i-1}}^\circ = x_{t_{i-1}}, \quad (1.4)$$

where  $\tilde{r}(t, x) = \nabla_x \log \tilde{\rho}(t, x)$  and  $\tilde{\rho}(t, x)$  is defined analogously to  $\rho(t, x)$ , by replacing the transition densities  $p$  with  $\tilde{p}$  in (1.3). If the laws of the processes  $X^\circ$  and  $X^*$  are absolutely continuous, then one can simulate from  $X^\circ$  instead of  $X^*$  and correct for the discrepancy between these processes using the Radon–Nikodym derivative of their induced laws on  $C([0, t_n])$ . As the SDE for  $X^\circ$  is obtained from the SDE for  $X$  by superimposing a guiding term, the paths distributed according to the former law are called *guided proposals*. The process  $X^\circ$  is typically used as a proposal in a Metropolis–Hastings step, where the terminology “proposal” stems from. However, our results can also be used in other Monte Carlo procedures, for example in an auxiliary particle filter. Furthermore, guided proposals can also be used to create flexible variational classes for latent diffusion paths.

## 1.3. Innovation

It is the purpose of this paper to show how to efficiently compute all of the non-trivial terms required for an implementation of guided proposals when the auxiliary diffusion  $\tilde{X}$  is chosen to solve a linear SDE. To this end, we derive simple systems of ordinary differential equations that can be used to compute all the relevant terms. These results imply that in order to sample paths of the proposal diffusion  $X^\circ$  and embed them in the Metropolis–Hastings algorithm only the following steps need to be performed

- a system of ordinary differential equations has to be solved backwards in time (suitable systems are given in Theorems 3.2, 3.3 and 3.4);

- paths of  $X^\circ$  need to be simulated forward in time, using standard simulation techniques based on stochastic Taylor expansions (cf. [Kloeden and Platen \(2013\)](#));
- the Radon–Nikodym derivative between the laws of  $X^*$  and  $X^\circ$  has to be evaluated and then used in the acceptance probability of the Metropolis–Hastings algorithm.

We call the resulting algorithm the *Backward Filtering Forward Guiding* (BFFG) algorithm, because (as we will show) it combines backward filtering under the auxiliary process  $\tilde{X}$  and forward simulation of the guiding process  $X^\circ$ . It may also be characterised as a variant of the forward filtering-backward sampling algorithm for linear state space models with (possibly) non-linear continuous time processes. Reversing the time-direction and sampling the process forward in time is not strictly necessary, but turns out to be more convenient.

For the smoothing problem, the first step needs to be executed only once and is akin to the updating equations in hybrid Kalman filtering. However, for the inference problem (in full generality) this same step needs to be repeated for each proposed value of the unknown parameter and hence its efficiency is of utmost importance.

The systems of ODEs introduced in this article make use only of the matrix addition, multiplication and inversion operations and scale much better to high dimensional problems compared to for example [van der Meulen and Schauer \(2017b\)](#).

The remaining two steps from the bullet-point list above are equally efficient as the first one—sampling proposal paths involves only samplers of unconditioned diffusions (in the numerical section of this article we rely on the Euler–Maruyama scheme) and in view of the fact that all of the terms needed for an evaluation of the Radon–Nikodym derivative are known upon solving the ODEs, the last step amounts to simple additions and multiplications. In fact, all three steps share the same order of complexity and hence simulation of any single proposal path  $X^\circ$  can be thought of as having similar order of cost as simulation of an unconditioned diffusion.

We believe the method derived in this paper has a number of attractive properties:

1. It is a computationally simple algorithm that provides a unified approach to smoothing of both hypo-elliptic and uniformly elliptic diffusions.
2. It allows for taking into account nonlinearities in the drift efficiently (by choice of the auxiliary process  $\tilde{X}$ ).
3. It can deal with a large class of diffusions with state-dependent diffusion coefficient.
4. The algorithm targets the exact smoothing distribution and does not rely on Gaussian approximations.
5. While our numerical examples are under the observation scheme as specified in [\(1.2\)](#), it can be adapted to nonlinear observation schemes or non-Gaussian error densities while still sampling from the exact smoothing distribution (cf. Section [4.3](#)).

Regarding the final point, we derive our algorithm in continuous time, but ultimately, in any implementation the SDE for  $X^\circ$  needs to be discretised. However, choosing the mesh-width for the discretisation can be controlled by the user.

We remark that there exist two standard techniques for improving the efficiency with which the Metropolis–Hastings algorithm explores a path space: the preconditioned Crank–Nicolson scheme (cf. [Cotter et al. \(2013\)](#) and [Beskos et al. \(2008\)](#)), in which the updates of the driving Wiener increments of the smoothed path are done via local perturbations; and blocking ([Shephard and Pitt, 1997](#)), in which one introduces artificial observations of the process  $X$

that, by the Markov property, allow to perform path imputation on shorter time segments. [van der Meulen and Schauer \(2017b\)](#) proposed a solution to the smoothing problem using diffusion bridges with fixed endpoints, spanning the two intervals between three consecutive observations and while taking the middle observation into account. However, this solution did not provide an efficient method for computing  $\tilde{\rho}(0, x_0)$ , a quantity that is required for parameter estimation. Furthermore, updating only short segments of the latent path can negatively affect the mixing time.

All of the above shortcomings are removed in this paper. In particular, regarding the restriction to blocking, any user-defined number of blocks of overlapping intervals (including the most extreme case consisting of a single block: i.e. the complete path  $\{X_t, t \in [0, t_n]\}$ ) can be handled at no extra overhead cost. For example, in Section 7.1 we show that for a partially observed Lorenz system removing the restriction on the block size leads to multiple orders of magnitude improvement in the overall computational cost.

#### 1.4. Outline

In Section 2 we recap previous work on guided proposals and explain which quantities need to be computed in their application to smoothing and parameter estimation. In Section 3 we derive ODE-systems for computing the guiding term in and relate them to linear continuous-discrete backward filtering. We provide an intuitive explanation for the derived formulas in Section 4. Next, the backward differential equations are used in the definition of our smoothing and parameter estimation algorithm in Section 5. In Subsection 5.3 we comment on the choice of the auxiliary process  $\tilde{X}$ . In Section 6 we address applications of the proposed algorithms to problems in which the dimension of the state-space of the diffusion is high. In such a setting, the backward filtering can for example be carried out using an ensemble Kalman filter. We illustrate our results on 3 challenging examples in Section 7. The appendix contains a derivation of the guiding term for guided proposals together with proofs of the main results. For backward filtering, the central results in this paper are Theorem 3.2, 3.3 (information filter) and 3.4 (covariance filter). These give systems of backward ordinary differential equations that can be used to derive all the necessary terms needed for an implementation of guided proposals in smoothing and inference.

## 2. Recap guided proposals

Here we recap some previous work on guided proposals:

- (A) In [Schauer et al. \(2017\)](#) the basic idea was introduced in the setting of uniformly elliptic diffusions (i.e. the case where for each  $y \in \mathbb{R}^d$  there exists an  $\varepsilon > 0$  such that  $\|\sigma(t, x)'y\| \geq \varepsilon\|y\|^2$ ), with one segment and a “full” observation at the time of conditioning. More precisely, the aim is to simulate a diffusion, conditioned on  $X_0 = x_0$  and  $X_T = x_T$ .
- (B) In [van der Meulen and Schauer \(2017b\)](#) this was extended to the setting of two future conditionings. More precisely, in this paper it was shown how to define guided proposals to sample from a diffusion starting in  $X_0 = x_0$  and conditioned on  $v_S \sim N(LX_S, \Sigma_S)$  and  $X_T = x_T$ , where  $0 < S < T$ .
- (C) In [Bierkens et al. \(2019\)](#) the work on [Schauer et al. \(2017\)](#) was generalised in a different direction by incorporating hypo-elliptic diffusions, observed partially and without noise.

More precisely, here it is assumed that  $X_0 = x_0$  and the conditioning is given by  $LX_T = v_T$ .

In all cases, the SDE for the conditioned process is of the form

$$dX_t^* = b(t, X_t^*) dt + a(t, X_t^*) r(t, X_t^*) dt + \sigma(t, X_t^*) dW_t \quad (2.1)$$

where  $r(t, x) = \nabla_x \log \rho(t, x)$ , that is to say, (2.1) determines the transition behaviour of the conditional process. Together with  $X_0^* \sim p^*$ , where  $p^*$  is the conditional density of  $X$  at time 0 given the observations, (2.1) gives the conditional process.

The function  $\rho$  is specific to the type of conditioning and depends on the unknown transition densities  $p$  of the diffusion  $X$ . In this paper, we consider  $\rho$  as specified in (1.3). The guided proposal process is in all cases defined as the (strong) solution to the SDE

$$dX_t^\circ = b(t, X_t^\circ) dt + a(t, X_t^\circ) \tilde{r}(t, X_t^\circ) dt + \sigma(t, X_t^\circ) dW_t, \quad X_0^\circ = x_0,$$

where  $\tilde{r}(t, x) = \nabla_x \log \tilde{\rho}(t, x)$  and  $\tilde{\rho}(t, x)$  is defined as  $\rho(t, x)$ , but with  $p$  replaced by the transition densities  $\tilde{p}$  of an auxiliary diffusion  $\tilde{X}$  (chosen to guarantee tractability of  $\tilde{p}$ ). The choice of the law of  $\tilde{X}$  impacts the quality with which the law of  $X^\circ$  approximates the law of the target process  $X^*$ . Intuitively, the drift and dispersion of  $\tilde{X}$  should be chosen such that  $\tilde{X}$  is similar to  $X$  in areas visited by the true conditional process; however, at the same time, the two functions need to be simple enough, so as to make it possible to compute  $\tilde{\rho}(t, x)$  and  $\tilde{r}(t, x)$ . Schauer et al. (2017) showed that the linear processes, defined by the SDE

$$d\tilde{X}_t = \left( \beta(t) + B(t)\tilde{X}_t \right) dt + \tilde{\sigma}(t) dW_t, \quad (2.2)$$

give rise to a family of auxiliary diffusions that grant a generous degree of flexibility for crafting suitable proposals  $X^\circ$ , while at the same time computations involving transition densities  $\tilde{p}$  remain tractable. Nonetheless, tractable is not synonymous with efficient.

Under boundedness and smoothness assumptions on the drift coefficient  $b$  and dispersion coefficient  $\sigma$  and additionally ‘‘matching conditions’’ (see Remark 2.1), it follows from Theorem 1 in Schauer et al. (2017) and Theorem 2.14 in Bierkens et al. (2019) that  $\mathbb{P}^*$  (the law of  $X^*$  starting in  $x_0$ ) is absolutely continuous with respect to  $\mathbb{P}^\circ$  (the law of  $X^\circ$  starting in  $x_0$ ) and

$$\frac{d\mathbb{P}^*}{d\mathbb{P}^\circ}(X^\circ) = \frac{\tilde{\rho}(0, x_0)}{\rho(0, x_0)} \Psi(X^\circ), \quad (2.3)$$

where

$$\Psi(X^\circ) = \exp \left( \int_0^T G(s, X_s^\circ) ds \right), \quad (2.4)$$

and

$$\begin{aligned} G(s, x) &= (b(s, x) - \tilde{b}(s, x))' \tilde{r}(s, x) \\ &\quad - \frac{1}{2} \text{tr} \left( [a(s, x) - \tilde{a}(s)] [H(s) - \tilde{r}(s, x) \tilde{r}(s, x)'] \right). \end{aligned} \quad (2.5)$$

Here  $\tilde{a}(s) = \tilde{\sigma}(s)\tilde{\sigma}(s)'$  and  $H(s)$  is the negative of the Hessian matrix of  $x \mapsto \nabla_x \log \tilde{\rho}(s, x)$  (which turns out not to depend on  $x$ ).

**Remark 2.1.** In setting (A), the matching condition is given by  $\tilde{a}(T) = a(T, x_T)$  which can always be ensured. In setting (C) the matching conditions are more subtle and more complicated. The results in Bierkens et al. (2019) strongly suggest that for the diffusivity of the auxiliary process the condition  $La(T, x_T)L' = L\tilde{a}(T)L'$  suffices. In case of hypo-ellipticity, additionally the drift of the auxiliary process,  $\tilde{b}(t, x) = B(t)x + \beta(t)$ , needs to satisfy the equation  $Lb(T, x_T) = L\tilde{b}(T, x_T)$ . These conditions are particularly important when the noise on the discrete time (partial) observations is small.

In practice, the guided proposal is forward simulated using a discretisation scheme for SDEs (such as Euler–Maruyama scheme). Then, the integral in (2.4) is evaluated using a quadrature rule. If some parameters in the drift or diffusion coefficient of  $X$  are unknown and it is desired to estimate them, evaluation of  $\tilde{\rho}(0, x_0)$  in (2.3) is also necessary. *To conclude, use of guided proposals requires efficient numerical evaluation of  $\tilde{r}$ ,  $H$  and  $\tilde{\rho}(0, x_0)$ .*

### 3. Differential equations for evaluating $\tilde{r}$ , $H$ and $\tilde{\rho}$

Our main results for the backward filtering step are Theorems 3.2, 3.3 and 3.4. All proofs are in Section B of the appendix. Let  $v(t)$  be defined by the concatenated vector of all non-past observations:

$$v(t) = [v'_i, \dots, v'_n]' \quad t \in (t_{i-1}, t_i],$$

where  $i \in \{1, \dots, n\}$ . Define  $v(0) = [v'_0, \dots, v'_n]'$ , let  $m(t) = \dim(v(t))$  and recall  $m_i = \dim(v_i)$ . Throughout we assume

**Assumption 3.1.** For each  $i \in \{0, \dots, n\}$ , the matrix  $\Sigma_i$  is strictly positive definite.

**Theorem 3.2.** Let the triplet  $(L(t), M^\dagger(t), \mu(t))$  be defined on each interval  $(t_{i-1}, t_i]$  ( $i = 1, \dots, n$ ) as solutions to the backward ODE systems

$$dL(t) = -L(t)B(t)dt \quad (3.1)$$

$$dM^\dagger(t) = -L(t)\tilde{a}(t)L(t)'dt \quad (3.2)$$

$$d\mu(t) = -L(t)\beta(t)dt. \quad (3.3)$$

At  $t = t_n$

$$L(t_n) = L_n \quad M^\dagger(t_n) = \Sigma_n \quad \mu(t_n) = 0$$

and for  $i = 0, \dots, n-1$ ,

$$L(t_i) = \begin{bmatrix} L_i \\ L(t_i+) \end{bmatrix}, \quad M^\dagger(t_i) = \begin{bmatrix} \Sigma_i & 0_{m_i \times m(t_i+)} \\ 0_{m(t_i+) \times m_i} & M^\dagger(t_i+) \end{bmatrix}, \quad \mu(S) = \begin{bmatrix} 0_{m_i \times d} \\ \mu(t_i+) \end{bmatrix}. \quad (3.4)$$

If  $M(t) = M^\dagger(t)^{-1}$ , then for all  $t \in [0, t_n]$ , we have

$$\begin{aligned} \tilde{r}(t, x) &= F(t) - H(t)x, \\ \tilde{\rho}(t, x) &= (2\pi)^{-m(t)/2} |M(t)|^{1/2} \exp(q_t(v(t), x)), \end{aligned}$$

where

$$H(t) = L(t)'M(t)L(t), \quad (3.5)$$

$$F(t) = L(t)'M(t)(v(t) - \mu(t)), \quad (3.6)$$

$$q_t(v, x) = -\frac{1}{2} (v - \mu(t) - L(t)x)' M(t) (v - \mu(t) - L(t)x).$$

Note that the equations for  $M^\dagger$  and  $\mu$  are not truly differential equations and that the values of  $M^\dagger(t)$  and  $\mu(t)$  can be found by using a numerical quadrature rule such as for example the trapezoid rule. This Theorem shows that  $H$  and  $\tilde{r}$  can be computed by solving the systems (3.1), (3.2) and (3.3). Additionally, by computing the term  $|M(t)|$ , we may evaluate  $\tilde{\rho}$  as well. In Theorem 3.3 below we will see that computation of this determinant can be avoided by solving another (scalar-valued) backward ODE.

The dimensions of the equations in Theorem 3.2 are larger on  $(t_{i-1}, t_i]$  than on  $(t_{j-1}, t_j]$  for all  $j > i$ . The dimension on the segment closest to zero (i.e. the leftmost segment) grows rapidly with a large number of observations. It turns out that other sets of backward differential equations can be derived, which are constant in dimensions determined by the the dimension of the state space of the diffusion, no matter the number of observations.

Throughout, we denote with  $\varphi(x; \mu, \Upsilon)$  the density of the  $N(\mu, \Upsilon)$ -distribution, evaluated at  $x$ .

**Theorem 3.3** (Information filter). For  $(t, x) \in [0, T] \times \mathbb{R}^d$ ,  $\tilde{\rho}$  admits the following decomposition

$$\log \tilde{\rho}(t, x) = -c(t) - \frac{1}{2}x'H(t)x + F(t)'x,$$

where on each interval  $(t_{i-1}, t_i]$  ( $i = 1, \dots, n$ ),  $H$ ,  $F$  and  $c$  solve the backward ODEs

$$\begin{aligned} dH(t) &= (-B(t)'H(t) - H(t)B(t) + H(t)\tilde{a}(t)H(t)) dt, \\ dF(t) &= (-B'(t)F(t) + H(t)\tilde{a}(t)F(t) + H(t)\beta(t)) dt, \\ dc(t) &= \left( \beta(t)'F(t) + \frac{1}{2}F(t)'\tilde{a}(t)F(t) - \frac{1}{2}\text{tr}(H(t)\tilde{a}(t)) \right) dt. \end{aligned}$$

At time  $t = t_n$  we have

$$H(t_n) = L_n'\Sigma_T^{-1}L_n, \quad (3.7)$$

$$F(t_n) = L_n'\Sigma_T^{-1}v_n, \quad (3.8)$$

$$c(t_n) = -\log \varphi(v_n; 0, \Sigma_n) \quad (3.9)$$

For  $i = 0, \dots, n-1$ ,

$$H(t_i) = H(t_i+) + L_i'\Sigma_i^{-1}L_i, \quad (3.10)$$

$$F(t_i) = F(t_i+) + L_i'\Sigma_i^{-1}v_i, \quad (3.11)$$

$$c(t_i) = c(t_i+) - \log \varphi(v_i; 0, \Sigma_i). \quad (3.12)$$

Note that  $H(t) \in \mathbb{R}^{d \times d}$ ,  $F(t) \in \mathbb{R}^d$  and that  $c(t)$  is scalar-valued throughout  $(0, T]$ .

**Theorem 3.4** (Covariance filter). Let  $\nu(t) = P(t)F(t)$  with  $P(t) = H(t)^{-1}$ . The mapping  $\tilde{r}$  satisfies

$$P(t)\tilde{r}(t, x) = \nu(t) - x, \quad (3.13)$$

On each interval  $(t_{i-1}, t_i]$  ( $i = 1, \dots, n$ ),  $P$  and  $\nu$  satisfy the backward ODEs

$$\begin{aligned} \frac{dP(t)}{dt} &= B(t)P(t) + P(t)B(t)' - \tilde{a}(t), \\ \frac{d\nu(t)}{dt} &= B(t)\nu(t) + \beta(t). \end{aligned} \quad (3.14)$$

At time  $t = t_n$  we have

$$P(t_n) = (L'_n \Sigma_n^{-1} L_n)^{-1} \quad \nu(t_n) = (L'_n \Sigma_n^{-1} L_n)^{-1} L'_n \Sigma_n^{-1} v_n.$$

For  $i = 0, \dots, n-1$ ,

$$P(t_i) = P(t_i+) - P(t_i+) L'_i (\Sigma_i + L_i P(t_i+) L'_i)^{-1} L_i P(t_i+) \quad (3.15)$$

$$\nu(t_i) = P(t_i) (L'_i \Sigma_i^{-1} v_i + H(t_i+) \nu(t_i+)). \quad (3.16)$$

In case  $\tilde{\sigma}$  and  $B$  are constant,  $P(t)$  can be computed more efficiently.

**Proposition 3.5.** Assume  $B$  and  $\tilde{a}$  are constant and  $\Sigma$  solves the continuous time Lyapunov equation

$$B\Sigma + \Sigma B' + \tilde{a} = 0.$$

Then the solution to

$$\frac{dP(t)}{dt} = BP(t) + P(t)B' - \tilde{a}, \quad P(T) = P_T$$

is given by

$$P(t) = \Phi(t, T)(\Sigma + P_T)\Phi(t, T)' - \Sigma, \quad (3.17)$$

where  $\Phi(t, T) = \exp(-(T-t)B)$ .

**Remark 3.6.** It is natural to ask which of the 3 recursions to use. In case of only one future observation at time  $t_1$ , the ODEs in Theorem 3.2 are advantageous when  $m_1 < d$ . Moreover, these are also applicable in case of a noiseless observation at time  $t_1$  by taking  $M^\dagger(t_1)$  to be equal to a zero matrix. With multiple observations, usually, the recursions from Theorem 3.3 or 3.4 are preferable and can lead to large computational gains.

In case  $L'_n \Sigma_n^{-1} L_n$  is not invertible,  $P(t_n)$  is not well-defined. This problem can be circumvented by equipping  $\tilde{X}_{t_n}$  with a proper prior distribution. In Section 4.2 we provide further details.

## 4. Backward Filtering Forward Guiding (BFFG)

In this section we give intuition on the proposed procedure. For  $t \geq 0$ , denote the set of non-past observations by  $\mathcal{V}_t$ , i.e.  $\mathcal{V}_t = \{V_i: t_i \geq t\}$ . With slight abuse of notation, set  $\mathcal{V}_i = \mathcal{V}_{t_i}$ .

### 4.1. Forward smoothing

Assume  $X_0$  is known and denote  $X_{t_i}$  by  $X_i$ . Suppose now we are interested in the smoothing distribution of  $(X_1, \dots, X_n)$ . It can be computed recursively from

$$p(X_1, \dots, X_i \mid \mathcal{V}_1) = p(X_i \mid X_{i-1}, \mathcal{V}_1)p(X_1, \dots, X_{i-1} \mid \mathcal{V}_1).$$

Here the first term on the right hand side captures the dynamics of the conditional process, which equals the product of the unconditional transition density  $p$  and a ratio of generalised transition densities

$$p(X_i \mid X_{i-1}, \mathcal{V}_1) = p(X_i \mid X_{i-1}, \mathcal{V}_i) = p(t_{i-1}, X_{i-1}; t_i, X_i)w_i,$$

where

$$w_i = \frac{p(\mathcal{V}_i \mid X_i)}{p(\mathcal{V}_i \mid X_{i-1})} = \exp(\log \rho(t_i, X_i) - \log \rho(t_{i-1}, X_{i-1})).$$

In a simplified view of our approach, in the first step we compute the filtering densities backward in time and in the second step we sample  $X_i \mid X_{i-1}$  and obtain the smoothing distribution by a change of measure, with weight  $w_i$ . One can now show using the arguments laid out in Appendix A that this expression is equal to the exponential process of a change of measure

$$\mathbb{E} \left[ \exp \left( \int_{t_{i-1}}^{t_i} \sigma(s, X_s)' \nabla \log \rho(s, X_s) dW_s - \frac{1}{2} \int_{t_{i-1}}^{t_i} \|\sigma(s, X_s)' \nabla \log \rho(s, X_s)\|^2 ds \right) \mid X_{i-1} \right],$$

which reveals the changed drift  $b + a \nabla \log \rho$  of the conditional process. Finally, instead of sampling a diffusion process with the drift  $b + a \nabla \log \rho$  we employ guided proposals as introduced in Section 2.

#### 4.2. Backward filtering

The interpretation of  $\nu$  and  $P$  (appearing in Theorem 3.4) follows from  $\tilde{X}_t \mid \mathcal{V}_t \sim N(\nu(t), P(t))$ , i.e. these are the mean and covariance of the backward filtered process. The update formula at observations times can now be seen from the following argument. Denote  $\tilde{X}_i \equiv \tilde{X}_{t_i}$ . Suppose  $(\nu(t), P(t))$  has been computed for  $t \in (t_i, t_n]$  for  $i \in \{0, \dots, n-1\}$ . At time  $t_i$  the observation  $\tilde{X}_i$  can be incorporated using the following relation:

$$p(\tilde{X}_i \mid \mathcal{V}_i) \propto p(V_i \mid \tilde{X}_i, \mathcal{V}_{i+1}) p(\tilde{X}_i \mid \mathcal{V}_{i+1}) = p(V_i \mid \tilde{X}_i) p(\tilde{X}_i \mid \mathcal{V}_{i+1}). \quad (4.1)$$

Since  $\tilde{X}_i \mid \mathcal{V}_{i+1} \sim N(\nu(t_i+), P(t_i+))$  and  $V_i \mid \tilde{X}_i \sim N(L_i \tilde{X}_i, \Sigma_i)$ , the joint distribution of  $(\tilde{X}_i, V_i) \mid \mathcal{V}_{i+1}$  is Normal. Hence there is a closed form expression for the distribution of  $\tilde{X}_i \mid (V_i, \mathcal{V}_{i+1})$  which gives  $\nu(t_i)$  and  $P(t_i)$ .

For  $i = n$ , note that  $p(\tilde{X}_n \mid V_n) \propto p(V_n \mid \tilde{X}_n) p(\tilde{X}_n)$ . If we assume  $X_n \sim N(\kappa, C)$ , we obtain

$$\begin{aligned} P(t_n) &= (L_n' \Sigma_n^{-1} L_n + C^{-1})^{-1}, \\ \nu(t_n) &= P(t_n)(L_n' \Sigma_n^{-1} v_n + C^{-1} \kappa). \end{aligned} \quad (4.2)$$

#### 4.3. Backward filtering for nonlinear observation schemes

Throughout we have assumed that  $V_i \sim N(L_i X_{t_i}, \Sigma_i)$ . This case is fully tractable for filtering and no approximation is made (except for discretisation errors that can be controlled by the user). However, tractability is lost when a more general scheme  $V_i \sim N(g_i(X_{t_i}), \Sigma_i)$  is considered. Thankfully, there is a host of methods for dealing with this case using approximate schemes. Note that in the BFFG-algorithm the observations only enter into the backward filtering equations, and only at observation times. More precisely, they only enter into the update step determined by (4.1).

If  $V_i \mid \tilde{X}_i$  does not have a normal distribution, one can find a Gaussian approximation to the joint law of  $(V_i, \tilde{X}_i)$  (Algorithm 5.1 in [Särkkä \(2013\)](#)), from which the conditional law of

$\tilde{X}_i \mid \mathcal{V}_i$  can be obtained. This simply boils down to an update step of the extended Kalman-filter (Algorithm 5.4 in [Särkkä \(2013\)](#)). We refer to Chapters 5 and 6 in [Särkkä \(2013\)](#) for other algorithms proposed in the literature. However, we now explain that even with Gaussian approximations the exact smoothing distribution can be targeted.

To this end, assume indeed that instead of  $V_i \sim N(L_i X_{t_i}, \Sigma_i)$  one observes  $V_i \sim N(g_i(X_{t_i}), \Sigma_i)$ . For incorporating  $V_i$  into the backward recursion, consider the linearisation

$$g_i(x) \approx g_i(\nu(t_i+)) + G_i(x - \nu(t_i+)) = \zeta_i + G_i x.$$

where  $G_i = (Dg_i)(\nu(t_i+))$  and  $\zeta_i = g_i(\nu(t_i+)) - G_i \nu(t_i+)$ . Under this linearisation, backward filtering can be carried out exactly as in our original setting by assuming to observe  $V_i - \zeta_i$  instead of  $V_i$  and setting  $L_i$  to be equal to  $G_i$ . As an approximation is made, the resulting backward filtering is inexact. Fortunately, in the forward guiding step we can correct for this by multiplying the change of measure in Equation (2.3) by

$$\prod_{i=1}^n \frac{\varphi(v_i; g_i(X_{t_i}^\circ), \Sigma_i)}{\varphi(v_i; \zeta_i + G_i X_{t_i}^\circ, \Sigma_i)}.$$

This correction term is similar to the one appearing in Theorem 3.3 in [van der Meulen and Schauer \(2017b\)](#).

Just like the guiding term under  $\tilde{X}$  is not the same as under  $X$ , the guiding term under the linearisation is not the same as under the nonlinear observation scheme. However, both approximations can be accounted for in the forward guiding step through the likelihood ratio. We stress that contrary to the the backward filtering, the forward guiding step does not involve linearisation of the SDE-dynamics. Non-Gaussian observation errors can be addressed in similar manner provided that the density of the error distribution is dominated by the Gaussian distribution.

## 5. A novel smoothing and parameter estimation algorithm

In this section we present a novel algorithm for continuous-discrete smoothing of diffusions. We initially assume  $\theta$  is known and  $x_0$  is fully observed. Suppose that at times  $t_1 < \dots < t_n$  realisations  $v_i$  of  $LX_{t_i} + \eta_i$  are observed. Anticipating later extensions of the algorithm with unknown parameters, we will use the subscript  $\theta$  at various places to highlight dependence of  $b$ ,  $\sigma$  or  $\Sigma_i$  on an unknown parameter.

As we assume existence of a strong solution to the SDE (1.4), there exists of a measurable map  $\mathcal{GP}_\theta$  such that

$$X = \mathcal{GP}_\theta(X_0, W),$$

where  $W$  is a Wiener process in  $\mathbb{R}^{d'}$ .

Below, we have used the information filter from Theorem 3.3. Clearly, with straightforward modifications it can be adjusted to other filtering equations from Section 3.

**Algorithm 5.1.** *Smoothing algorithm for fixed  $\theta$  and initial state  $x_0$ .* Choose a persistence parameter  $\lambda \in [0, 1)$  and a Markov kernel  $q_\theta$  for updating the initial state. Denote the number of MCMC iterations by  $N$ .

1. **Compute the guiding term.** Initialise

$$\begin{aligned} H(t_n) &= L'_n \Sigma_n^{-1} L_n, \\ F(t_n) &= L'_n \Sigma_n^{-1} v_n, \\ c(t_n) &= -\log \varphi(v_n; 0, \Sigma_n). \end{aligned}$$

For  $i = n - 1$  to 0

(a) For  $t \in (t_i, t_{i+1}]$ , backwards solve the ordinary differential equations

$$\begin{aligned} dH(t) &= (-B(t)' H(t) - H(t)B(t) + H(t)\tilde{a}(t)H(t)) dt, \\ dF(t) &= (-B'(t)F(t) + H(t)\tilde{a}(t)F(t) + H(t)\beta(t)) dt, \\ dc(t) &= \left( \beta(t)' F(t) + \frac{1}{2} F(t)' \tilde{a}(t) F(t) - \frac{1}{2} \text{tr}(H(t)\tilde{a}(t)) \right) dt, \end{aligned}$$

(b) Compute

$$\begin{aligned} H(t_i) &= H(t_i+) + L'_i \Sigma_i^{-1} L_i, \\ F(t_i) &= F(t_i+) + L'_i \Sigma_i^{-1} v_i, \\ c(t_i) &= c(t_i+) - \log \varphi(v_i; 0, \Sigma_i). \end{aligned}$$

2. **Initialise the path.** Sample a Wiener process  $Z$  on  $[0, t_n]$ . Compute a corresponding guided proposal  $X^\circ = \mathcal{GP}_\theta(x_0, Z)$ , via

$$dX_t^\circ = b(t, X_t^\circ) dt + a(t, X_t^\circ) (F(t) - H(t)X_t^\circ) dt + \sigma(t, X_t^\circ) dZ_t.$$

Initialise  $X$  by defining  $X = (X_t^\circ, t \in [0, t_n])$ .

3. **MCMC steps.** Repeat  $N$  times

(a) Sample independently a Wiener process  $W$  and set

$$Z^\circ = \lambda Z + \sqrt{1 - \lambda^2} W.$$

Compute

$$X^\circ = \mathcal{GP}_\theta(x_0, Z^\circ).$$

(b) Compute  $A = \Psi_\theta(X^\circ)/\Psi_\theta(X)$ , where  $\Psi$  is as defined in (2.4). Draw  $U \sim \mathcal{U}(0, 1)$ . If  $U < A$  set  $X = X^\circ$  and  $Z = Z^\circ$ .

For computing the guiding term,  $H(t)$  and  $F(t)$  are calculated on  $t \in [t_0, t_n]$ ; the formulas follow directly from Theorem 3.3. Once these have been calculated and stored (on a fine grid), the remainder of the algorithm consists of preconditioned Crank–Nicolson steps on the Wiener increments. After “burnin”, the sample paths generated by this algorithm are from the smoothing distribution. Note that since we assume the initial state  $x_0$  to be known and the parameter  $\theta$  to be fixed,  $c(t)$ , in fact, does not need to be computed. As we will shortly extend the presented algorithm to include uncertainty over the initial state and parameter estimation we have already included the ODE and the update formula for  $c(t)$ .

While Algorithm 5.1 is theoretically valid for any fixed value of  $\lambda$ , its efficiency strongly depends on the particular choice of this parameter. Instead of a fixed value of  $\lambda$ , we can choose it randomly at each iteration of step (3a): the acceptance probability in step (3b) is not affected by its value (cf. the discussion after Algorithm 1 in [van der Meulen and Schauer \(2017a\)](#)).

**Remark 5.2.** In case of absence of noise on some of the observation's coordinates, matrices  $\Sigma_i$ ,  $i \in \{1, \dots, n\}$  become singular. In such instances,  $\Sigma_i$ 's can be approximated with  $\tilde{\Sigma}_i = \Sigma_i + \epsilon I_{m_i}$  for some *small*  $\epsilon > 0$  and the update equations from Theorem 3.3 can be computed accordingly, with  $\tilde{\Sigma}_i$  in place of  $\Sigma_i$ .

**Remark 5.3.** If the measurement error is close to zero, then the (Euler) discretisation of the guided proposal is a delicate matter due to the behaviour of the guiding term just prior to observation times. As discussed in Section 5 of [van der Meulen and Schauer \(2017a\)](#) a time change and scaling of the process can alleviate discretisation errors. For completeness, we present this approach in appendix C.

### 5.1. Initial state updating

In case the initial state is not fully observed, a separate step can be included for updating it. In this case, it is necessary to evaluate  $\tilde{\rho}_\theta(0, x_0)$ . This value can be obtained from Theorem 3.3, which implies that

$$\log \tilde{\rho}_\theta(0, x_0) = -c_\theta(0) - \frac{1}{2}x_0' H_\theta(0)x_0 + F_\theta(0)'x_0. \quad (5.1)$$

Recall  $\pi$  denotes the density of  $X$  at time 0 (the prior density of  $X_0$ ).

**Algorithm 5.4.** *Initial state updating step.* Suppose current parameter value  $\theta$ , innovations  $Z$  and starting point  $x_0$  such that  $X = \mathcal{GP}_\theta(x_0, Z)$ . Choose a Markov kernel  $q$  for proposing a new state  $x_0^\circ$ .

1. Propose  $x_0^\circ$  from the proposal kernel  $q$ .
2. Compute the corresponding guided proposal  $X^\circ = \mathcal{GP}_\theta(x_0^\circ, Z)$ .
3. Compute

$$A = \frac{\pi(x_0^\circ) \tilde{\rho}_\theta(0, x_0^\circ)}{\pi(x_0) \tilde{\rho}_\theta(0, x_0)} \frac{\Psi_\theta(X^\circ)}{\Psi_\theta(X)} \frac{q_\theta(x_0^\circ | x_0)}{q_\theta(x_0 | x_0)},$$

where  $\Psi$  is as defined in (2.4). Draw  $U \sim \mathcal{U}(0, 1)$ . If  $U < A$  set  $x_0 = x_0^\circ$ .

The initial state can be initialised by sampling from the  $N(H(0)^{-1}F(0), H(0)^{-1})$  distribution, which is the distribution of  $X_0$  conditioned on all observations under the law of the auxiliary process  $\tilde{X}$ . This follows directly from Equation (5.1). Alternatively, one can simply set it to the mean of this distribution, that is, by solving  $H(0)x_0 = F(0)$ .

Note that initialisation rules for  $(\nu(T), P(T))$  (or equivalently  $(F(T), H(T))$ ) can be understood as variants of the generic update rules (3.16) and (3.15) using  $H(T+) = 0$ . Instead, one can initialise  $\nu(T+)$  and  $P(T+)$  with given mean and covariance using these rules.

Then Algorithm 5.4 with modified acceptance rate

$$A\varphi(X_T, \nu(T+), P(T+))/\varphi(X_T^\circ, \nu(T+), P(T+))$$

can be used while preserving the exact smoothing distribution.

### 5.2. Parameter updating

In case there are unknown parameters in either the drift or dispersion coefficient, or if the covariance matrices  $\Sigma_i$  ( $0 \leq i \leq n$ ) cannot be assumed known, then a data augmentation

algorithm can be used. This entails iteratively sampling from the unknown parameters conditional on the smoothed path, followed by the presented smoothing algorithm with the current values of the parameters. This approach is well known in the present setting and goes back to the seminal paper by [Roberts and Stramer \(2001\)](#). For a general discussion on this we refer to [van der Meulen and Schauer \(2017a\)](#).

**Algorithm 5.5.** *Parameter updating step.* Suppose current iterate  $\theta$  and  $X = (X_t, t \in [0, t_n])$ , where  $X = \mathcal{GP}_\theta(x_0, Z)$ . Choose a Markov kernel  $q$  for proposing new value for  $\theta$ .

1. Propose  $\theta^\circ$  from the proposal kernel  $q$ .
2. Compute the corresponding guided proposal  $X^\circ = \mathcal{GP}_{\theta^\circ}(x_0, Z)$ .
3. Compute

$$A = \frac{\tilde{\rho}_{\theta^\circ}(0, x_0)}{\tilde{\rho}_\theta(0, x_0)} \frac{\Psi_{\theta^\circ}(X^\circ)}{\Psi_\theta(X)} \frac{q(\theta | \theta^\circ)}{q(\theta^\circ | \theta)},$$

where  $\Psi$  is as defined in (2.4). Draw  $U \sim \mathcal{U}(0, 1)$ . If  $U < A$  set  $\theta = \theta^\circ$ .

The following Gaussian conjugacy result is sometimes useful; its proof is an elementary consequence of Girsanov's theorem.

**Proposition 5.6.** Assume a diffusion  $X$  with drift of the form

$$b(t, x) = \varphi_0(t, x) + \sum_{k=1}^K \theta_k \varphi_k(t, x)$$

and diffusion coefficient independent of  $\theta$ . If the full path  $(X_t, t \in [0, T])$  is observed and a priori  $\theta \sim N(0, \Gamma_0^{-1})$ , then  $\theta | X \sim N(\Gamma^{-1}\mu, \Gamma^{-1})$  with

$$\mu = \int_0^T \Phi(t, X_t)' a^{-1}(t, X_t) (dX_t - \varphi_0(t, X_t) dt),$$

$$\Gamma = \int_0^T \Phi(t, X_t)' a^{-1}(t, X_t) \Phi(t, X_t) dt + \Gamma_0,$$

where  $\Phi(t, x) = (\varphi_k(t, x))_{1 \leq k \leq K}$ .

### 5.3. Choice of the auxiliary process $\tilde{X}$

The auxiliary process  $\tilde{X}$  needs to be chosen by a user, i.e. the parameters  $\beta(t)$ ,  $B(t)$  and  $\tilde{\sigma}(t)$  need to satisfy matching and regularity conditions, but are otherwise free. A number of practical ways for choosing them are discussed in [van der Meulen and Schauer \(2017a\)](#) (Section 4.4); below, we list a number of reasonable options. Determining an optimal auxiliary law in an automated fashion deserves its own study and is the subject of an ongoing research (but cf. also considerations in [Schauer et al. \(2017\)](#)).

**A** Waive the freedom and simply take  $\tilde{\sigma}$  constant,  $B(t) \equiv 0$  and  $\beta = 0$ . If  $X$  is either elliptic or hypo-elliptic with nonzero noise on each coordinate, this yields a valid algorithm. It still takes local nonlinearity into account through the presence of  $b$  in (1.4) and, in case of partial observations, is informed by multiple future observations.

**B** On each  $t \in (t_{i-1}, t_i]$  compute a first order Taylor expansion of the drift evaluated at a specified  $\tilde{x}(t_i)$ . That is, compute  $\tilde{b}(t, x) = b(t, \tilde{x}(t_i)) + J_b(t, \tilde{x}(t_i))(x - \tilde{x}(t_i))$ , where  $J_b$  denotes the Jacobian matrix of  $b$ . In case the diffusion is fully observed,  $\tilde{x}(t_i)$  is taken equal to  $X_{t_i}$ , else it is specified by a user-chosen guess for it. The guess can be adaptively refined by using empirical averages of the imputed path. Otherwise put, the auxiliary process comes from linearisations of the target diffusion at the times of subsequent observations.

**C** The aim is to employ a first order Taylor expansion  $\tilde{b}(t, x) = b(t, \bar{x}(t)) + J_b(t, \bar{x}(t))(x - \bar{x}(t))$  evaluated at  $\bar{x}(t) = \mathbb{E}[X_t | D]$ . Of course,  $\bar{x}(t)$  is unknown, but information becomes available during MCMC-iterations, and thus, just as in **B**, empirical averages of the imputed path can be used as its proxy. More specifically, we propose to first use the auxiliary process constructed by one of the preceding methods to get  $B^{(0)}(t, x) = \beta(t) + B(t)x$ , and then, run the algorithm for  $k$  iterations and compute the average of these  $k$  paths. Denote this average by  $\{\bar{X}^{(0)}(t), t \in [0, t_n]\}$ . Next, starting at  $i = 1$ , repeat the following steps until the prescribed total number of iterations for adaptation has been reached.

(a) Set

$$B^{(i)}(t, x) = b(t, \bar{X}^{(i-1)}(t)) + J_b(t, \bar{X}^{(i-1)}(t)) \left( x - \bar{X}^{(i-1)}(t) \right).$$

(b) Recompute  $H(t)$ ,  $F(t)$  and  $c(t)$  on  $[0, t_n]$  based on  $B^{(i)}(t, x)$ .

(c) Perform  $k$  MCMC-iterations based on  $H(t)$ ,  $F(t)$  and  $c(t)$ . Compute the average of all simulated paths to obtain  $\{\bar{X}^{(i)}(t), t \in [0, t_n]\}$

To avoid common problems with adaptive schemes we stop the adaptation after a fixed number of steps.

**D** Choose  $\tilde{\sigma} = \sigma$ ,  $B(t) \equiv 0$  and take  $\beta$  nonzero to make the pulling term itself take into account the nonlinearity of the system. To determine  $\beta$ , first obtain  $F(t_n)$  and  $H(t_n)$  as in step 1 of Algorithm 5.1. Next, for  $i = n$  to 1:

(a) For  $t \in (t_{i-1}, t_i]$ , backwards solve

$$dx(t) = b(t, x(t)) dt, \quad x(t_i) = H(t_i)F(t_i).$$

Set  $\beta(t) = b(t, x(t))$ .

(b) Using  $\beta$ , compute  $(F(t), H(t))$  for all  $t \in (t_{i-1}, t_i]$ . Compute  $(F(t_{i-1}), H(t_{i-1}))$  using  $(F(t_{i-1}+), H(t_{i-1}+))$  using the formulas in step 1b of Algorithm 5.1.

**E** Use a linear combination of the schemes above. This is a risk-averse strategy, which aims to guard against unexpected artifacts that some of the adaptive strategies above might exhibit (say, for strategy **C** such behaviour could appear as a result of multimodality on a path space). In the numerical section below we use:  $B = wb^{(C)} + (1-w)b^{(D)}$ , where  $b^{(C)}$  and  $b^{(D)}$  are defined by strategies **B** and **C** respectively and  $w \in [0, 1]$  are some user-chosen weights. Another option (not considered here) consists of sampling  $w$  in each iteration from the Bernoulli distribution with fixed success probability.

**F** Finally, the auxiliary process may take values in a higher dimensional space, with only its first  $d$  coordinates used in defining the proposal diffusion. Say, we want to target a process  $X$  conditioned on the observations  $V_i = LX_{t_i} + \eta_i$ . Consider an auxiliary process  $[\tilde{X}, Y]$  with  $\tilde{X}$  solving  $d\tilde{X}_t = (B\tilde{X}_t + \beta(t) + CY_t) dt + \tilde{\sigma} dW_t$  and  $Y$  a second, independent linear process  $dY_t = DY_t dt + dW_t^Y$  driven by an independent Brownian motion  $W^Y$ . Here  $B, C$  and  $D$  are matrices of suitable dimension. Then, we may use an

augmented sampler that targets the joint process  $[X_t, Y_t]$  conditional on the observations  $V_i$ . The augmented observation operator is given by  $L_{aug} = [L \ 0]$ , the augmented drift for the target process is  $b_{aug}(t, [x, y]) = [b(t, x), Dy]$  and the block diagonal dispersion coefficient is  $[\sigma \ 0 \ 0 \ I]$ ; the sampler uses the augmented guided proposal with the auxiliary linear process  $[\tilde{X}, Y]$  that has a drift  $\tilde{b}_{aug}(t, [x, y]) = [Bx + Cy, Dy]$  and the block diagonal dispersion coefficient  $[\sigma \ 0 \ 0 \ I]$ . Samples of the conditional process  $X$  are obtained by marginalisation. To give a simple example,  $\tilde{X}$  can be taken to be a sum of a Brownian motion and an integrated Brownian motion.

#### 5.4. Blocking strategy

In this article, for comparisons of the effects of blocking we always adopt a “chequerboard” updating strategy. More precisely, we say that we use “blocks of length  $k$ ” (for an even  $k$ ) to mean that the following strategy is adopted for updating the path:

1. Initialise  $X_{(0:n)}$ .
2. For  $i = 1, \dots, \lfloor n/k \rfloor$ , sample bridges  $X_{(ki-k:ki)}$ , conditional on  $X_{ki-k}, X_{ki}$  and  $\{V_{ki-j}; j = 1, \dots, k-1\}$ .
3. Sample the last segment  $X_{(\lfloor n/k \rfloor k:n)}$  conditional on  $X_{\lfloor n/k \rfloor k}$  and  $\{V_j; j = \lfloor n/k \rfloor k, \dots, n\}$ .
4. For  $i = 1, \dots, \lfloor n/k \rfloor - 1$ , sample bridges  $X_{(ki-k/2:ki+k/2)}$ , conditional on  $X_{ki-k/2}, X_{ki+k/2}$  and  $\{V_{ki+j}; j = -k/2 + 1, \dots, k/2 - 1\}$ .
5. Sample the first segment  $X_{(0:k/2)}$  conditional on  $X_0, X_{k/2}$  and  $\{V_j; j = 1, \dots, k/2\}$ .
6. Sample the last segment  $X_{(\lfloor n/k \rfloor k-k/2:n)}$  conditional on  $X_{\lfloor n/k \rfloor k-k/2}$  and  $\{V_j; j = \lfloor n/k \rfloor k-k/2 + 1, \dots, n\}$ .

For each step of parameter update we perform either imputation steps 2 and 3 or 4–6.

## 6. Continuous-discrete smoothing for high dimensional diffusion processes

For high dimensional SDEs with  $d \gg 1$ , the computation of the  $d \times d$  backward filtered covariance  $P(t)$  in (3.13) becomes prohibitive in an implementation in dense matrix algebra (and likewise the equations for its inverse). Another numerical difficulty is the computation of the likelihood accounting for the difference in  $a$  and  $\tilde{a}$  in case these are unequal. In this section we do not consider the latter problem, and therefore, restrict our attention to the high dimensional situation where  $a = \tilde{a}$ . In this case the linear filtering step is the numerical bottleneck and not the sampling step. Specifically, if the process  $X$  and the observations are of the form

$$\begin{aligned} dX_t &= (B(t)X_t + F(t, X_t)) dt + \sigma_t dW_t, \quad X_0 \sim p(x_0), \\ Y_i &= LX_{t_i} + \eta_i, \quad \eta_i \sim N(0, \Sigma_i), \end{aligned} \tag{6.1}$$

then a natural choice is to take  $\tilde{B}(t) = B(t)$  and  $\tilde{\sigma}(t) = \sigma(t)$ .

Even if  $\tilde{B}$  and  $\tilde{\sigma}$  are sparse,  $P(t)$  typically is not. But if those operators that describe the drift and dispersion of  $\tilde{X}$  are *local*, then one may be able to approximate  $P$  by a sparse matrix. Instead of stating a formal definition we provide an illustrative example, which can be seen as a variant of the stochastic heat equation on a graph with drift. Consider the  $d$ -dimensional diffusion  $(X_t)$  for which a state  $x$  is understood as a discrete approximation to a function

$f: [0, 1] \rightarrow \mathbb{R}$ , so that in particular, a coordinate  $X^{(i)}$  corresponds to an evaluation of  $f$  in  $\frac{i-1}{d-1} \in [0, 1]$ . More concretely, let  $X$  be defined as a solution to

$$dX_t = -\frac{\sigma^2}{2}(\Lambda + cI)X_t dt + \sigma dW_t, \quad (6.2)$$

with  $\sigma, c > 0$  and

$$\Lambda = \begin{bmatrix} 1 & -1 & & & \\ -1 & 2 & -1 & & \\ & \ddots & \ddots & \ddots & \\ & & -1 & 2 & -1 \\ & & & -1 & 1 \end{bmatrix}, \quad (6.3)$$

the graph Laplacian of the linear graph with  $d$  vertices corresponding to the coordinates.  $\Lambda$  acts as a discrete approximation to the second derivative.  $\Lambda$  is a local operator in the sense of having a representation by a banded matrix (this corresponds to all interactions in the linear graph being limited to only those between the neighbours). As a result, matrix-vector operations (matvecs)  $\Lambda x$  can be computed efficiently in  $\mathcal{O}(d)$  time.  $X$  is a Gauss–Markov process with stationary distribution  $N(0, (\Lambda + cI)^{-1})$  (as  $\Sigma = (\Lambda + cI)^{-1}$  is a solution to the continuous time Lyapunov equation  $B\Sigma + \Sigma B' + C = 0$ , where  $B = -\sigma^2/2(\Lambda + cI)$ ). Thus, in the stationary regime,  $X(t)$  at a fixed time  $t$  is a draw from a high-dimensional Gaussian law approximating a spatial Gaussian process on  $[0, 1]$  with continuous realisations of Hölder regularity just below  $\frac{1}{2}$ . While  $(\Lambda + cI)^{-1}$  is not a sparse matrix, the entries decay exponentially moving away from the diagonal. By Proposition 3.5, the same holds for  $P(t)$ . Good, sparse approximations are obtained by setting  $(\Lambda + cI)^{-1}$  or  $P(t)$  to zero outside of a fixed band.

In contrast, the forward simulation and the likelihood evaluation happen in  $\mathbb{R}^d$  and are fast, as long as fast matvec operations with the operator  $H$  are available. This implies that the actual bottleneck of our approach is in solving a continuous-discrete linear filtering problem and we can rely on a long sequence of work in this direction.

From the various possibilities we consider but two: a sampling approach related to the ensemble Kalman filter and a sparsity enforcing solver for (3.14).

### 6.1. Ensemble backward filter

Instead of solving (3.14) one can exploit that for the linear backward process with a reversed time axis

$$d\bar{X}_s = (\bar{B}(s)\bar{X}_s + \bar{\beta}(s)) ds + \bar{\sigma}(s) d\bar{W}_s, \quad \bar{X}_0 \sim N(\nu_{t_{i+1}}, P_{t_{i+1}})$$

for  $T - s \in (t_i, t_{i+1})$  with  $\bar{B}(s) = -\tilde{B}(T - s)$ ,  $\bar{\beta}(s) = -\tilde{\beta}(T - s)$  and  $\bar{\sigma}(s) = \tilde{\sigma}(T - s)$ , it holds

$$\mathbb{E}[\bar{X}_s] = \nu(T - s) \quad \text{and} \quad \text{Var}(X_s) = P(T - s).$$

Here,  $d\bar{W}_s$  can be taken to be an Itô integral; as  $\tilde{\sigma}$  does not depend on space, there is no need for an Itô correction.

This can be used to obtain estimates of  $\nu(s)$  and a low rank approximation of  $P(s)$  by sampling  $\bar{X}^{(k)}$  a number of  $K$  times with  $K \ll d$  and approximating by the empirical covariance  $\Sigma = \frac{1}{K-1} \sum \bar{X}_{T-s}^{(k)} \bar{X}_{T-s}^{(k) \top}$ . To obtain a positive definite (and invertible) estimate of  $P$ , one employs localisation and sets  $\hat{P} = \Sigma \circ \Lambda$  where  $\circ$  is the Hadamard (elementwise) product with a positive definite sparse localisation matrix  $\Lambda$  chosen to ignore long range dependencies, see

[Houtekamer and Mitchell \(2001\)](#). The observations are taken into account by way of the usual ensemble Kalman filter

$$\bar{X}_{T-t_i}^{(k)} = X_{T-t_i+}^{(k)} + \hat{P}(t+)L_i' \left( L_i \hat{P}(t+)L_i' + \Sigma \right)^{-1} (v_i - L_i X_{T-t_i+}^{(k)}),$$

see [Evensen \(2003\)](#).

### 6.2. Forced sparsity

Secondly, we consider sparsity enforcing backward integrators, where we set

$$P(t-h) = \text{drop}_\epsilon \left( P(t) + (-\tilde{B}(t)P(t) - P(t)\tilde{B}(t)' + \tilde{a}(t))h \right).$$

Here

$$(\text{drop}_\epsilon A)_{ij} = \begin{cases} A_{ij} & |A_{ij}| > \epsilon \\ 0 & \text{otherwise} \end{cases}.$$

If  $P$  is well-approximated by a sparse matrix – as illustrated for the case (6.2) – then  $\text{drop}_\epsilon P_h$  will be sparse. We explore this approach in Subsection 7.3.

**Remark 6.1.** A particularly relevant case of (6.1) is a process  $X$  that is obtained from a spatial discretisation of the stochastic partial differential equation

$$d\mathbb{X}_t = (-\mathbf{A}\mathbb{X}_t + \mathbf{F}(t, \mathbb{X}_t)) dt + \boldsymbol{\sigma}_t d\mathbb{W}_t, \quad \mathbb{X}_0 = \mathbf{x}_0, \quad (6.4)$$

taking solutions in a Hilbert space  $\mathbb{H}$ , where  $\mathbf{A}$  is a densely defined, positive definite operator and  $\mathbb{W}$  is a  $\mathbf{Q}$ -Wiener process with a covariance operator  $\mathbf{Q}$  given by a positive definite trace class operator, see [Da Prato and Zabczyk \(2014\)](#).

## 7. Examples

In all examples, the differential equations for  $H(t)$ ,  $F(t)$  and  $c(t)$  have been solved using the 7th order Runge–Kutta solver (cf. [Verner \(1978\)](#)). The guided proposal is obtained by solving its SDE using Euler discretisation. The code is available in the folders `scripts/papers` of the package `BridgeSDEInference.jl` ([Mider et al. \(2019\)](#)) and `scripts` of the package `BridgeSPDE.jl`. Both packages build upon [Schauer and contributors \(2017\)](#), for the programming language Julia ([Bezanson et al. \(2017\)](#)).

### 7.1. Lorenz system

The Lorenz system is notable for having chaotic solutions for certain parameter values and initial conditions. It is described by the SDE with the drift and dispersion coefficient given by

$$b(x) = \begin{bmatrix} \theta_1(x_2 - x_1) \\ \theta_2x_1 - x_2 - x_1x_3 \\ x_1x_2 - \theta_3x_3 \end{bmatrix} \quad \text{and} \quad \sigma = \sigma_0 I_{3 \times 3}.$$

**Data:** We initialised the process at  $x_0 = [1.5 \ -1.5 \ 25]'$  and simulated it on  $[0, 2]$  with mesh-width 2e-4 and parameters  $\theta = [10 \ 28 \ 8/3]', \sigma_0 = 3$ . Only the 2nd and 3rd coordinate were observed so that  $L_i$  is a  $2 \times 3$  matrix with the first row  $[0, 1, 0]$  and the second row  $[0, 0, 1]$ . We then defined two datasets.

**Dataset 1:** 200 observations were retained at times  $0.01, 0.02, \dots, 2$ , where we took  $\Sigma_i = 5 \cdot I$  as the covariance matrix for the noise.

**Dataset 2:** 10 observations were retained at times  $0.2, 0.4, \dots, 2$ , where we took  $\Sigma_i = 0.05 \cdot I$ . The observed data are shown in Figures 1 and 2. Note that the first coordinate process  $\{X_{1,t}; t \in [0, T]\}$  remains latent in both cases.

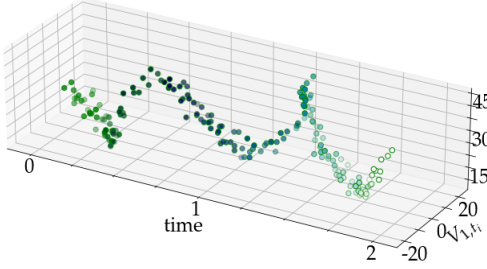


FIGURE 1. Dataset 1

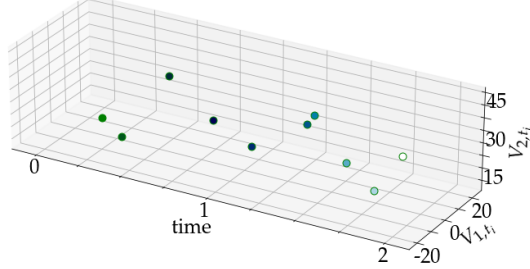


FIGURE 2. Dataset 2

**Algorithm details:** Overall, six inference algorithms have been run, three on each dataset. The procedures were inferring parameter  $\theta$ , whereas parameter  $\sigma_0$  was assumed to be known. All four parameters could have been inferred simultaneously; however, by fixing  $\sigma_0$  it was possible to illustrate the differences in performances of various algorithms more clearly. Indeed, a varying  $\sigma_0$  locally influences the speed at which chains on a path space, as well as parameter chains mix and this makes it more difficult to disentangle the contribution due to efficiency of the algorithm from that of a locally elevated or decreased volatility. We illustrate the problem of inference for the volatility coefficient on a more challenging example in the following section.

We ran the following algorithms:

- Dataset 1
  - The algorithm of [van der Meulen and Schauer \(2017b\)](#). It is a special case of the algorithm proposed in this article, in which a path—instead of being imputed in full—is updated in blocks of length 2, as described in Section 5.4.
  - Inference algorithm with blocking, with blocks of length 8.
  - Inference algorithm with no blocking (where each proposal path is imputed in full).
- Dataset 2
  - Inference algorithm with no blocking.
  - Inference algorithm with blocks of length 2.
  - Inference algorithm with blocks of length 2 and adaptation of proposals laws.

We set the following Gaussian priors over the parameter  $\theta$  and the value of the starting point:

$$\theta \sim N(0, \text{diag}(10^3, 10^3, 10^3)), \quad X_0 \sim N(x_0, \text{diag}(400, 20, 20)).$$

Setting a Gaussian prior over  $\theta$  made it possible to implement conjugate updates for  $\theta$  (cf. Proposition 5.6 or [Van der Meulen et al. \(2014\)](#)). Each block had its own persistence parameter  $\lambda_i$  of the preconditioned Crank–Nicolson scheme (in case of no-blocking a single parameter  $\lambda$  was used). For each block,  $\lambda_i$  was tuned adaptively so as to target the acceptance probability of the imputation step for a given block to be 0.234 (cf. Section 3 of [Roberts and Rosenthal \(2009\)](#)). The updates of the initial position were always done jointly with the updates of the path in the first block (or jointly with the entire path updates in case of no blocking).

We chose the auxiliary process according to the strategy **B**, where the initial guess for  $\tilde{x}(t_i)$  was taken to be  $[\Xi_i \ v_{i,1} \ v_{i,2}]'$ ,  $\Xi_i = 25$ ,  $(i = 1, \dots, n)$ , and where the values of  $\Xi_i$  were updated over the course of running an MCMC sampler: during the first 2500 iterations, once in every 500 steps we used an empirical average of  $X_{1,t_i}$  to re-define  $\Xi_i$ . Note that this was done in all six experiments.

Additionally, in the experiment with the “adaptation”, we used strategy **E**, where the adaptation time was set to 2500 iterations and adaptation updates were done once in every 500 steps. The weights were changed from, initially, (1, 0) (the first value representing the weight for strategy **B**, the second one for strategy **C**), through (0.7, 0.3) and (0.4, 0.6) up to (0.2, 0.8) at iteration 1500 (from then on the weights remained unchanged).

We set the density of the imputation grid to  $2 \cdot 10^{-4}$ . The simulations took respectively: 784s, 570s, 198s, 137s, 260s and 777s to complete on an i5-5250U CPU, 1.60GHz.

**Results:** The results of the experiments associated with the first dataset are shown in Figure 3 and they illustrate the outcome of only the first  $10^4$  iterations. The summary concerning time-adjusted effective sample size that is based on the entire chain is given in Table 1.

The green dashed lines in the top-most three traceplots indicate the values taken by the diffusion trajectory that was used to produce the data. As we only have one realisation of the path and finitely many observations, the conditional distribution (given the data) is not centred at this line; however, we can expect the samples to be close to them. The green dashed lines in the bottom three traceplots indicate the values of the parameters that were set to simulate the data.

Under the first observational setting the discrepancy between an approximate and a true guiding term is small and thus blocking becomes a hindrance that decelerates mixing of the parameter chains and the path chain. This is clearly illustrated in the left-most column of Figure 3, which corresponds to the algorithm of [van der Meulen and Schauer \(2017b\)](#), where the block-length is set to 2. By increasing the block-length to 8 (centre column) the mixing is improved and by removing it altogether and updating the entire path at once even better mixing can be achieved (right column). The same conclusions are strongly supported by the results summarised in Table 1, where the difference in the time-adjusted effective sample size is in excess of 2 orders of magnitude (we used function `ESS` implemented in R to compute the effective sample size).

In the top row of Figure 3 we plotted a thinned chain of the imputed trajectories (1 in every 100 sampled paths is given; note that unlike Figures 1 and 2, the temporal component is represented only by the changing colour of the trajectories, whereas each of the three axes have purely spatial meaning and correspond to the coordinates of the process  $X$ ). Notice how short blocks cause a slowdown in mixing on a path space, effectively disallowing the sampler to perform large moves. This is expected to be of a particular hindrance to sampling of multimodal diffusions.

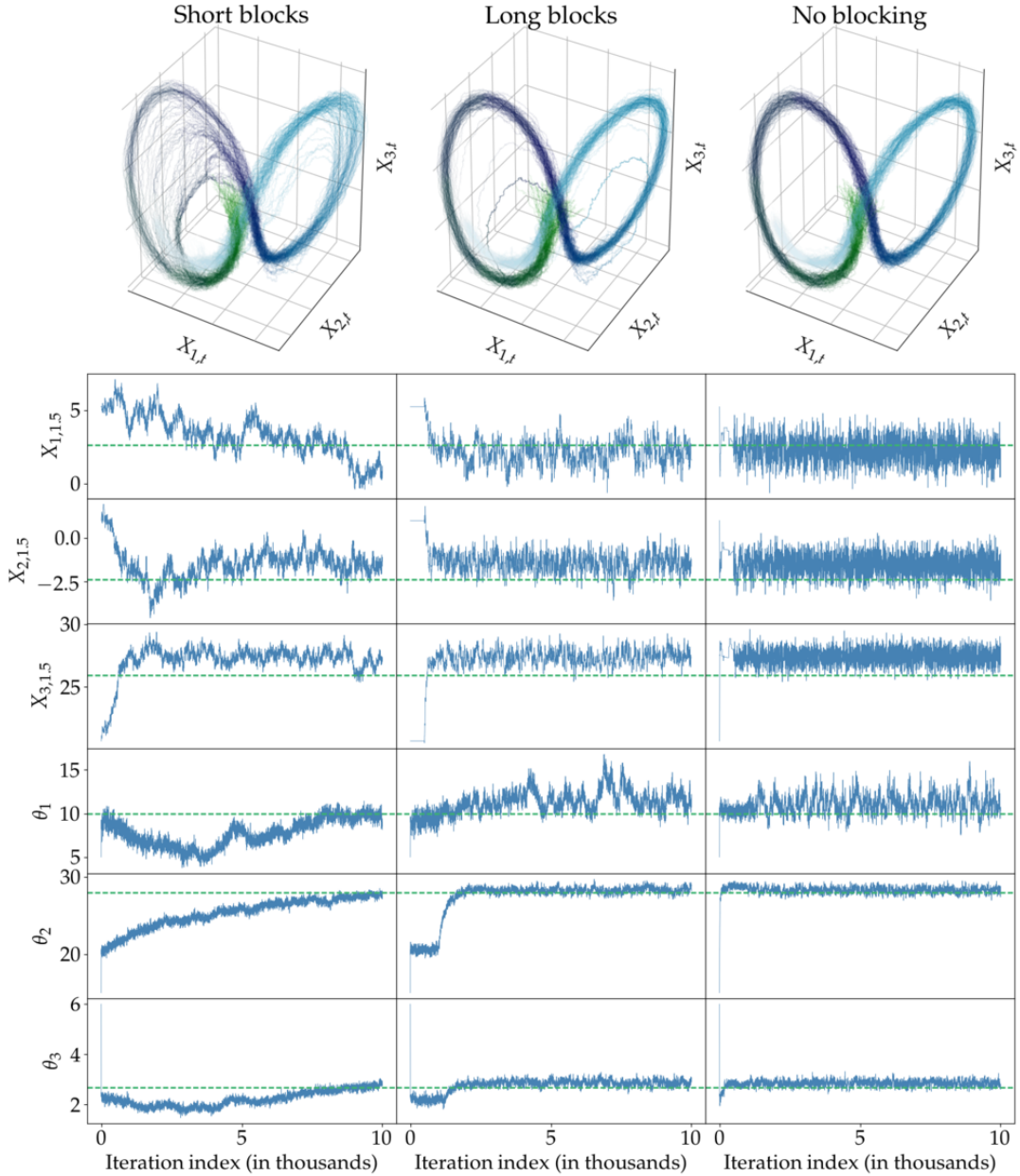


FIGURE 3. Lorenz system: results on **dataset 1**. Left column: results of a single MCMC run with blocks set to comprise of two inter-observation intervals (as in [van der Meulen and Schauer \(2017b\)](#)); middle column: blocks comprising of eight inter-observation intervals; right column: no blocking. Top plots: paths sampled by the MCMC samplers (1 in every 100 sampled paths); Rows 2–4: marginal distribution of the coordinates of  $X$  at time  $t = 1.5$ . Rows 5–7: traceplots for the updated parameters  $\theta$ .

taESS (ESS)			
	short blocks	long blocks	no blocking
$X_{1,1.5}$	0.164 (128.6)	1.991 (1134.9)	<b>52.932 (10480.3)</b>
$X_{2,1.5}$	0.447 (350.1)	5.164 (2943.4)	<b>115.610 (22890.5)</b>
$X_{3,1.5}$	0.545 (427.0)	1.468 (836.6)	<b>121.568 (24070.2)</b>
$\theta_1$	0.039 (30.6)	1.643 (936.6)	<b>23.194 (4592.4)</b>
$\theta_2$	0.081 (63.7)	0.366 (208.6)	<b>77.675 (15379.5)</b>
$\theta_3$	0.057 (44.5)	3.108 (1771.7)	<b>55.141 (10917.7)</b>

TABLE 1

Time-adjusted effective sample size (taESS) and effective sample size (ESS) for the experiments with the first dataset of the Lorenz example. Based on chains of length  $10^5$ . Best results are written in bold.

The results from the first dataset clearly illustrate that removing the restriction on the block length can have a positive effect on the efficiency of sampling on a path space. Nonetheless, some caution must be executed in extrapolating those conclusions. To see this, consider the second dataset. It is qualitatively different from the first one, in that the inter-observation distance is large enough for the non-linear dynamics of the target process to become pronounced between any two observations, whereas the decreased observational noise elevates the impact of the guiding term (for this reason it is also considered to be a substantially more difficult problem, for which a smaller number of numerical schemes can be applied to).

The inference results obtained on the second dataset are gathered in Figure 4. In this setting, using blocking yields similar results as imputing the path in full. In fact, as summarised by Table 2, the values of taESS corresponding to parameter chains are approximately twice as large when blocking is used (as compared to a no-blocking scheme). However, it is possible to improve the mixing of the chains even further—as depicted in the centre column of Figure 4—by designing better proposal laws. We used a scheme from E simply to motivate the usefulness of making the coefficients of the auxiliary diffusion time-dependent. The topic of optimal choice of the auxiliary law is beyond the scope of this paper.

Problems encountered in practice might fall anywhere on the spectrum spanned by the two datasets above or exhibit peculiarities of its own. We therefore believe that removing restriction on the block length—as it is done in this article—is a particularly practical improvement.

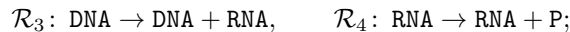
For reference we also ran the algorithm on the second dataset with the choice of the simplest strategy A and reported the result in Table 2.

## 7.2. Prokaryotic auto-regulatory gene network

We consider a simplified model of the auto-regulated protein transcription studied in Golightly and Wilkinson (2005, 2011). It is based on the stochastic model describing  $\lambda$  repressor protein cI of phage  $\lambda$  in Escherichia coli introduced in Arkin et al. (1998). The simplified model is characterised by eight biomolecular reactions: the reversible repression of transcription in which a protein dimer  $P_2$  attaches to certain sites on the DNA:



the transcription of DNA into mRNA and the subsequent translation and protein folding:



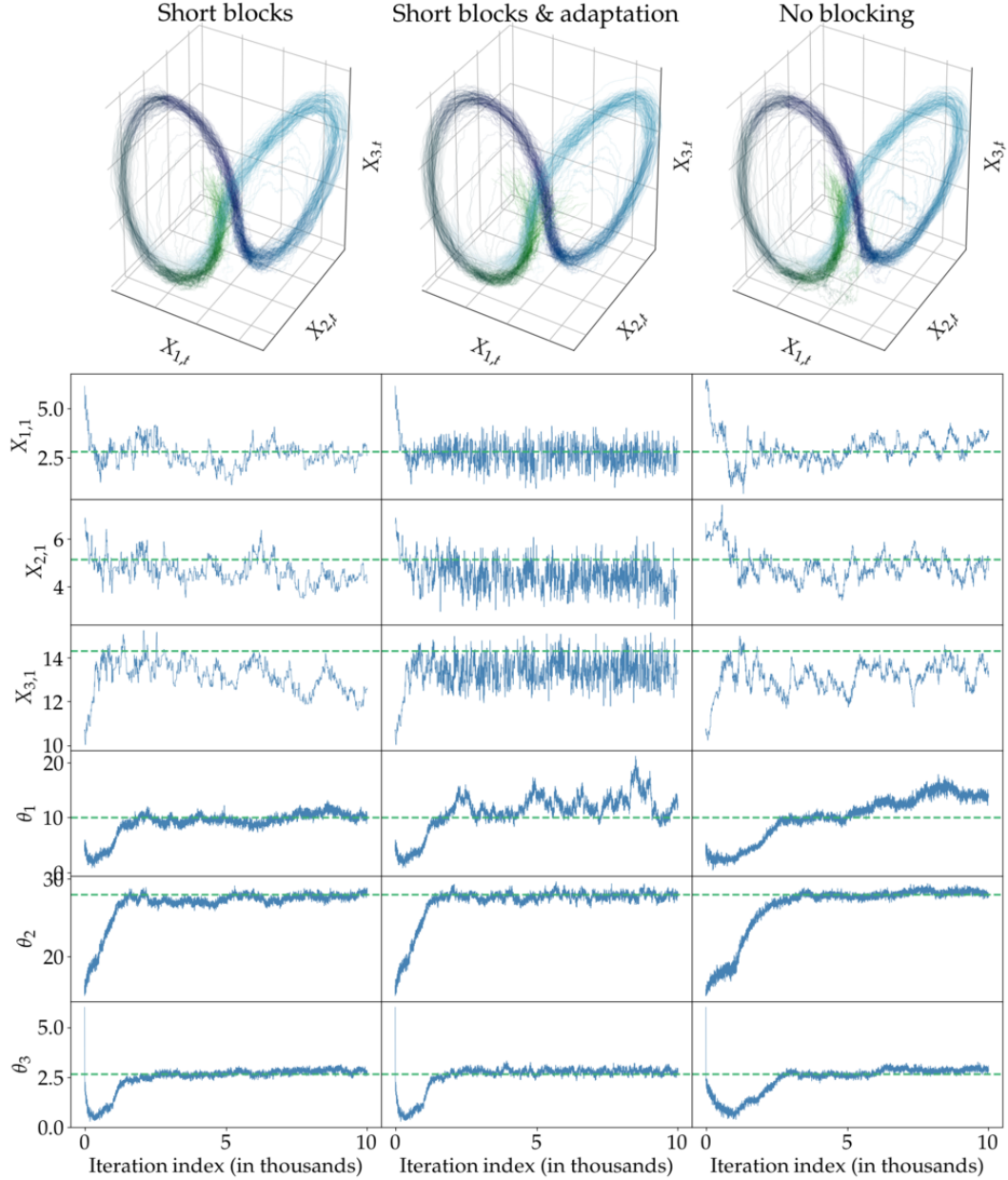


FIGURE 4. Lorenz system: results on **dataset 2**. Left column: results of a single MCMC run with no blocking; middle column: blocks comprising of two inter-observation intervals; right column: blocks of length 2 and adaptive tuning of the auxiliary law according to  $b^{(\text{aux})} = wb^{(7.1)} + (1-w)b^{(C)}$  (see Section 5.4 for details). Top plots: paths sampled by the MCMC samplers (1 in every 100 sampled paths); Rows 2–4: marginal distribution of the coordinates of  $X$  at time  $t = 1$ . Rows 5–7: traceplots for the updated parameters  $\theta$ .

	taESS (ESS)			
	short blocks	short blocks & adpt	no blocking	strategy <b>A</b>
$X_{1,1}$	1.328 (332.1)	<b>4.140 (3216.6)</b>	1.271 (175.3)	1.17 (56.2)
$X_{2,1}$	1.566 (391.4)	<b>5.162 (4011.0)</b>	1.618 (223.3)	0.600 (28.8)
$X_{3,1}$	1.366 (341.2)	<b>4.608 (3580.4)</b>	1.469 (202.7)	0.346 (16.5)
$\theta_1$	0.416 (103.9)	<b>0.602 (467.5)</b>	0.280 (38.6)	0.330 (15.8)
$\theta_2$	<b>1.307</b> (326.8)	0.963 ( <b>748.5</b> )	0.589 (81.2)	0.901 (43.3)
$\theta_3$	<b>0.76</b> (190.6)	0.563 ( <b>437.2</b> )	0.488 (67.3)	0.196 (9.39)

TABLE 2

Time-adjusted effective sample size (taESS) and effective sample size (ESS) for the experiments with the second dataset of the Lorenz example. Additional comparison for the experiments with the auxiliary law chosen according to the strategy **A**. Based on chains of length  $10^5$ . Best results are written in bold.

the reversible protein dimerisation:

$$\mathcal{R}_5: 2P \rightarrow P_2, \quad \mathcal{R}_6: P_2 \rightarrow 2P;$$

and the mRNA and protein degradation:

$$\mathcal{R}_7: RNA \rightarrow \emptyset, \quad \mathcal{R}_8: P \rightarrow \emptyset.$$

The total number of DNA strands is assumed to be fixed:  $DNA + DNA \cdot P_2 = K$ . It is well known that such system admits a diffusion approximation (called the chemical Langevin equation) and for the given system above, an associated SDE is given by:

$$dX_t = S(\theta \circ h(X_t)) dt + S \odot \gamma(\theta \circ h(X_t)) dW_t, \quad t \in [0, T], \quad X_0 = x_0,$$

where  $\circ: \mathbb{R}^d \times \mathbb{R}^d \rightarrow \mathbb{R}^d$  is a component-wise multiplication:

$$(\mu \circ \nu)_i = \mu_i \nu_i, \quad i = 1, \dots, d,$$

the operation  $\odot: \mathbb{R}^{d \times d'} \times \mathbb{R}^{d'} \rightarrow \mathbb{R}^{d \times d'}$  is defined via:

$$(M \odot \mu)_{i,j} = M_{i,j} \mu_j, \quad i = 1, \dots, d; j = 1, \dots, d',$$

the function  $\gamma: \mathbb{R}^d \rightarrow \mathbb{R}^d$  is a component-wise square root:

$$(\gamma(\mu))_i = \sqrt{\mu_i}, \quad i = 1, \dots, d,$$

$S$  is the stoichiometry matrix:

$$S = \begin{bmatrix} 0 & 0 & 1 & 0 & 0 & 0 & -1 & 0 \\ 0 & 0 & 0 & 1 & -2 & 2 & 0 & -1 \\ -1 & 1 & 0 & 0 & 1 & -1 & 0 & 0 \\ -1 & 1 & 0 & 0 & 0 & 0 & 0 & 0 \end{bmatrix},$$

and the function  $h$  is given by:

$$h(x) = (x_3 x_4, K - x_4, x_4, x_1, x_2(x_2 - 1)/2, x_3, x_1, x_2)'.$$

For this SDE  $X_t = (\text{RNA}_t, \text{P}_t, (\text{P}_2)_t, \text{DNA}_t)$  and  $W$  is an 8-dimensional Brownian motion. For more details about the model and how to derive chemical Langevin equations see [Golightly and Wilkinson \(2005\)](#).

We simulated three datasets using the Gillespie algorithm. In all three cases the process was started from  $x_0 = (8, 8, 8, 5)$  and we set  $K = 10$ .

**Dataset 1:** First, we reproduced the observational scheme of [Golightly and Wilkinson \(2011\)](#), where noisy estimates of the total number of proteins that are not attached to any DNA strands are recorded at integer times:

$$V_i = \begin{bmatrix} 0 & 1 & 2 & 0 \end{bmatrix} X_i + \eta_i, \quad \eta_i \sim N(0, 2^2), \quad i = 1, \dots, 100. \quad (7.1)$$

**Dataset 2:** Next, in addition to observations from (7.1), we assumed that for each 8 observations of protein counts it is possible to obtain one noisy count of RNA, i.e. that:

$$V_i = \begin{bmatrix} 1 & 0 & 0 & 0 \\ 0 & 1 & 2 & 0 \end{bmatrix} X_i + \eta_i, \quad \eta_i \sim N\left(0, \begin{bmatrix} 1^2 & 0 \\ 0 & 2^2 \end{bmatrix}\right), \quad i = 8, 16, \dots, 96, \quad (7.2)$$

and that for  $i \in \{1, 2, \dots, 100\} \setminus \{8, 16, \dots, 96\}$ ,  $V_i$  is given by (7.1).

**Dataset 3:** Finally, we took the second dataset and permuted the noisy RNA counts randomly. More precisely, if  $V_i^{(j)}$  denotes the  $i^{th}$  observations from the  $j^{th}$  dataset ( $i = 1, \dots, 100$ ;  $j = 2, 3$ ) then:

$$V_i^{(3)} = \begin{cases} V_i^{(2)}, & i \in \{1, 2, \dots, 100\} \setminus \{8, 16, \dots, 96\}, \\ \begin{bmatrix} V_{1,\zeta(i)}^{(2)} & V_{2,i}^{(2)} \end{bmatrix}, & i \in \{8, 16, \dots, 96\}, \end{cases}$$

with  $\zeta(i)$  denoting the  $i$ -th element of a random permutation  $\zeta$  of  $\{8, 16, \dots, 96\}$ .

**Algorithm details:** We ran the inference algorithm using guided proposals without blocking. Note that due to a rectangular shape of the volatility coefficient it is impossible to employ guided proposals with blocking and a non-zero persistence parameter  $\lambda$  of the preconditioned Crank–Nicolson scheme. Consequently, one can employ the algorithm of [van der Meulen and Schauer \(2017b\)](#) only in a special case when the observations are made on a sufficiently dense time-grid, for which it is possible to set  $\lambda = 0$ .

We set the prior distribution over the starting position to be  $X_0 \sim N(x_0, I_{4 \times 4})$  and, following [Golightly and Wilkinson \(2011\)](#), a prior distribution over the logarithm of each inferred parameter to be  $\text{Unif}([-7, 2])$ . We remark that the priors chosen by [Golightly and Wilkinson \(2011\)](#) that truncate the natural support of the parameters might be problematic, especially for the first dataset, as the data is not informative enough to narrow down the support of some of the posteriors, causing the parameter chains to hit against the boundaries of the priors. Instead, using an exponential prior over each  $\theta_i$ —this being the maximum entropy distribution of all continuous distributions supported on  $[0, \infty)$ —might be a more suitable choice. For the sake of fair comparison we stick with the choice made by [Golightly and Wilkinson \(2011\)](#).

The MCMC sampler started off with updating each log-transformed parameter separately using Metropolis–Hastings algorithm with random walk proposals and adaptation as described in Section 3 of [Roberts and Rosenthal \(2009\)](#). After the first  $12 \cdot 10^3$  steps of parameter updates we computed the empirical covariance of the parameter chains and switched to joint proposals of [Haario et al. \(2001\)](#) (we used a modified version from Section 2 of [Roberts and Rosenthal](#)

(2009)). We kept updating the empirical covariance matrix once in every 100 steps of the algorithm. We chose the auxiliary law according to the strategy **B**, where during the first  $10^4$  iterations of the Markov chain we updated our guesses for the latent positions of the path at the observation times once in every 200 iterations.

**Results:** Figure 5 summarises the results from running inference on each of the three datasets. For each log-transformed parameter we give traceplots of the Markov chain and the resulting marginal density plots (with burn-in set to  $2 \cdot 10^4$  iterations). The true parameter values are marked with orange, dashed, horizontal lines, whereas grey, dotted, vertical lines mark the change in the type of the transition kernel used (from adaptive, single-site updates to joint updates of Haario et al. (2001)).

For the dataset 1 we fixed  $\theta_5$ ,  $\theta_6$  and  $K$  to their true values and we aimed at inferring the remaining parameters. This is the same setup as in Golightly and Wilkinson (2011). The results are given in the left column of Figure 5.

Note that the marginal posteriors over  $\log(c_3)$  and  $\log(c_8)$  presented in Golightly and Wilkinson (2011, Figure 3) (corresponding to  $\log(\theta_3)$  and  $\log(\theta_8)$ ) concentrate decisively around incorrect values of the parameters, possibly pointing to some undiagnosed problems with the methodology. In our case, the true values of the parameters that were used to generate the data lie within the support of the posterior. In particular, the posteriors over  $\log(\theta_3)$  and  $\log(\theta_7)$  do not depart much from the priors, indicating that the data is not informative enough to identify those two parameters. Indeed, an examination of the reaction equations reveals that  $\theta_3$  and  $\theta_7$  regulate the production and the degradation of the RNA respectively and the observation scheme that provides only noisy counts of P might not provide sufficient information.

We generated the second dataset to examine the degree of improvement in identifying the true parameters that could be brought about by adding sparse observations of the RNA. We assumed that only  $K$  is known and we fixed  $\theta_6$  to an *incorrect* but *reasonable* value of  $\theta_6^* = 0.5$ . This was done to reproduce a real setting in which none of the  $\theta$  parameters are known, so fixing any  $\theta_i$  parameter to its true value is impossible. By fixing  $\theta_6$  to an incorrect value and running the inference algorithm we hope to estimate  $\theta_5/\theta_6$ . Ideally, one would want to estimate all 8 parameters simultaneously, but the dataset is not informative enough to conduct such inference. The results are summarised in the middle column of Figure 5. Parameters  $\theta_i$ ,  $i \in \{1, 2, 3, 4, 7, 8\}$  have been successfully identified and the posterior over  $\theta_5$  concentrates around the value  $\theta_5^*$  for which  $\theta_5^*/\theta_6^*$  is equal to the true ratio  $\theta_5/\theta_6$  of the parameters that were used to generate the data.

Naturally, the problem with the observational setting of dataset 2 is that noisy counts of  $\text{RNA}_t$  need not be easily available in practice. However, it is conceivable that it is possible to collect information about the marginal distribution of RNA. To make use of such information, at each time  $t \in \{8, 16, \dots, 96\}$  instead of observing a true, noisy count of  $\text{RNA}_t$  we could instead observe a realisation from the marginal density of RNA. We reproduce such observational setting by randomly permuting the time-labels of the generated  $\text{RNA}_t$ ,  $t \in \{8, 16, \dots, 96\}$ , resulting in the dataset 3. The inference results in this setting (assuming  $K$  known and  $\theta_6$  fixed to an incorrect value of  $\theta_6^* = 0.5$ ) are summarised in the right column of Figure 5. Some of the marginal posteriors appear flatter than the ones in the middle column, but the loss of information is not substantial and the posteriors still identify the true parameter values.

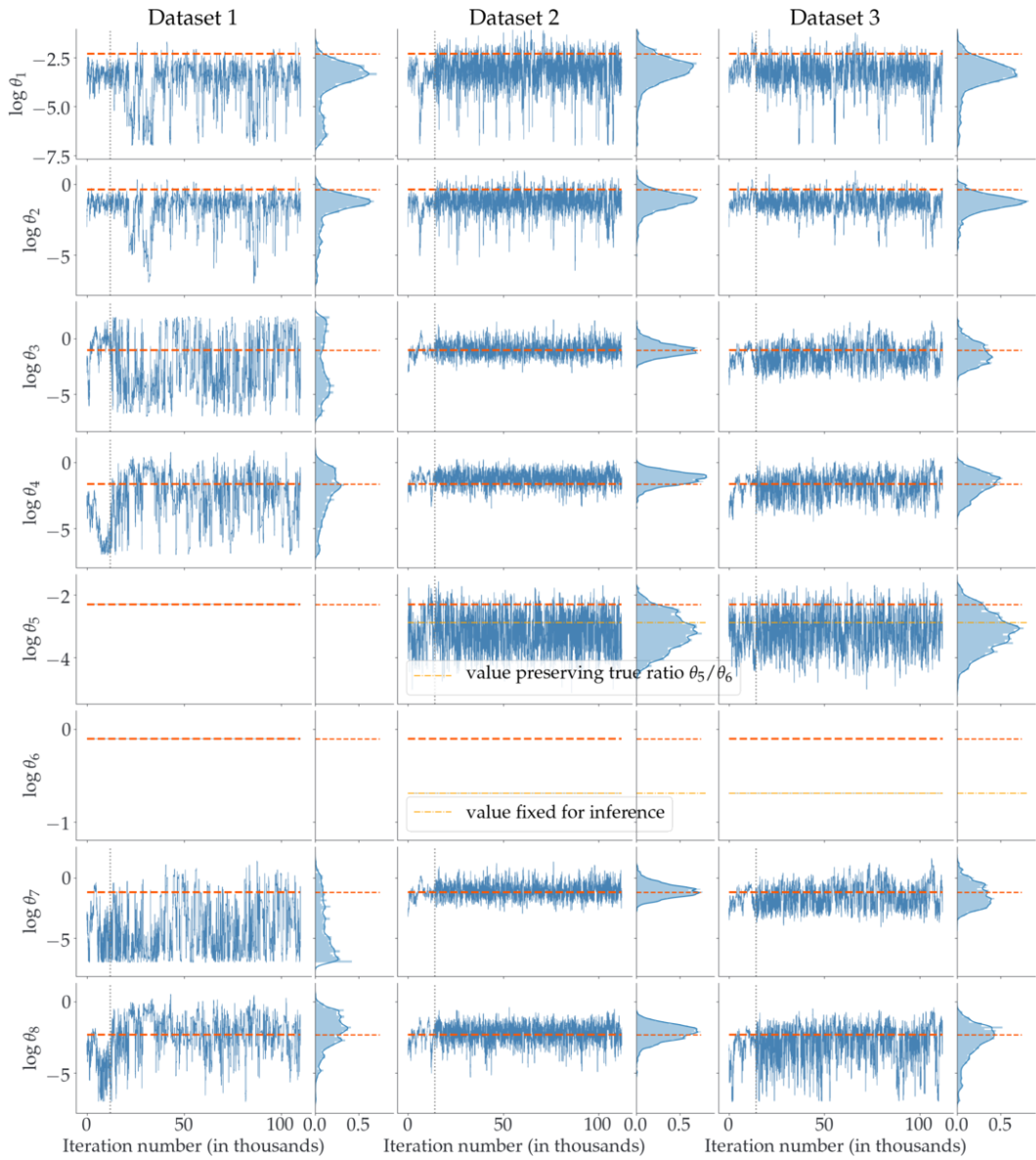


FIGURE 5. *Inference results for the prokaryotic example. Each iteration refers to a single step of parameter update. Left column gives the results of inference run on dataset 1; middle column: results from dataset 2; right column: results from dataset 3*

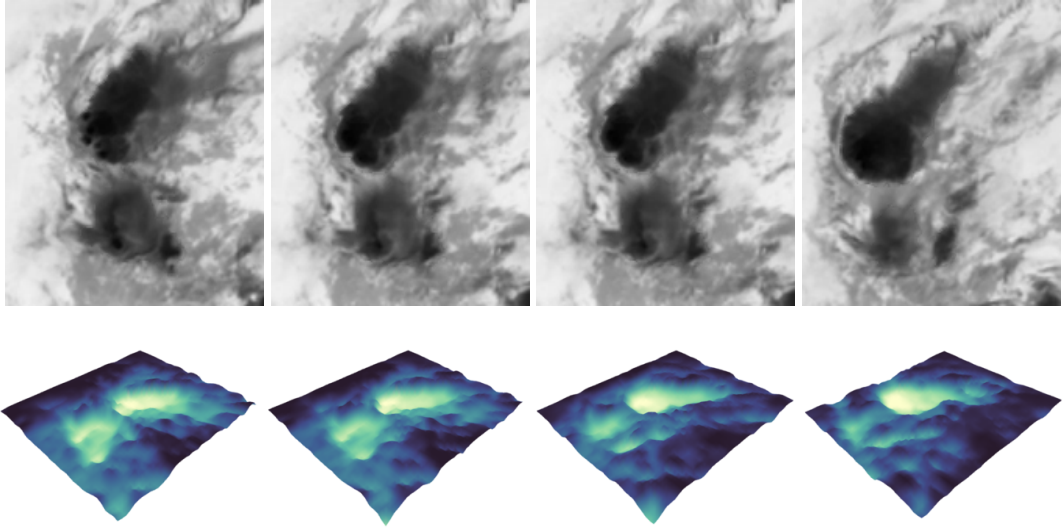


FIGURE 6. Sequence of infrared Meteosat-MSG2 satellite images depicting the evolution of a convective cloud system. Image from ([Avenel et al., 2014](#)).

### 7.3. Tracking the translation of a dynamic Gaussian random field

We consider the problem of inferring a latent spatial process from noisy low frequency observations. As an example we take a few pictures from a sequence of satellite images depicting the evolution of a convective cloud system taken 15 minutes apart. The sequence was analysed by [Avenel et al. \(2014\)](#) from the perspective of curve tracking.<sup>1</sup> A visual inspection indicates that the system moves south-east and we are interested in estimating the speed of the system, as well as its location and extent at intermediate times.

No attempt is made to physically model a convective system. This example is merely meant to serve as a starting point for applications in high dimensional settings. The statistical analysis is made on the minimalistic assumptions that we observe a large scale phenomenon moving at constant speed through space, but the images show additional temporal and spatial high frequency phenomena we consider as random and it is the latent, large scale evolution that we are interested in. In this way we develop a generic model to track deformations and translations in time not bound to this particular meteorological example. Both Wiener and formal observation noise then capture all dynamics, observation errors and local physical phenomena which cannot be explained by our simple model.

We set this numerical experiment up in the way of a 2-d generalisation of (6.2). It is convenient to describe the model as a discretely observed, matrix-valued Langevin process (stochastic heat equation) on the graph with a stationary distribution that shows large scale variation in the distribution of its samples. This is similar in spirit to [Hartog and van Zanten \(2019\)](#), but we take a more dynamical view with discrete time observations and continuous latent dynamics and a drift term. Furthermore, via forward guiding our approach has a natural non-Gaussian extension. To avoid working with covariance tensors describing the uncertainty of a matrix valued process we move to the equivalent, vector-valued process, obtained through

---

<sup>1</sup>The images were processed to remove annotated curves.

the application of the `vec` (vectorisation) operation.

The images have a single channel with values in  $[0, 1]$ , so each pixel corresponds to one entry of a real  $m \times n$  matrix, but we do not take the boundedness into account and model them as real-valued matrices. The matrix-valued observations are denoted by  $Y_0, \dots, Y_3$  corresponding to pictures with indices 33, 35, 40, 45. The chosen images are not equally spaced in time, but this poses no difficulty to our method. The last three pictures are taken 75 minutes apart, the first two pictures are 30 minutes apart. We consider 75 min as 1 time unit. The original image size was  $196 \times 166$  and it was downsampled to  $65 \times 55$ .

We assume that

$$Y_i = X_{t_i} + \eta_i, \eta_i \sim N(0, \Sigma),$$

where  $\eta$  is matrix-valued Gaussian noise with covariance tensor  $\Sigma$  of the appropriate dimension (corresponding to the covariance matrix of  $\text{vec}(\eta)$ ). We took  $\Sigma = \sigma_\epsilon^2 I$

The latent process is a stochastic process  $X = (X_t)$  as well taking values in the set of  $m \times n$ -real matrices, so nominally a 3575 dimensional diffusion process solving

$$dX_t = -\frac{\sigma^2}{2}(\rho\Lambda + cI)X_t dt + F_\theta(X_t) dt + \sigma dW_t, \quad (7.3)$$

with  $W_t$  an uncorrelated, matrix-valued Brownian motion,  $\sigma, \rho, c > 0$  and  $\Lambda$  the graph Laplacian tensor defined in (7.4) below.

The pixel indices  $i, j$  are identified with the vertices  $V = \{(i, j), i \in \{1, \dots, m\}, j \in \{1, \dots, n\}\}$  of the  $m \times n$ -lattice  $(V, E)$  with edges  $E = \{\{v, v'\} : v = (i, j), v' = (i', j') \in V, |i - i'| + |j - j'| = 1\}$  (using the set notation for edges). Thus, edges connect a pixel to its vertical and horizontal neighbours. Then

$$\Lambda_{v,v'} = \begin{cases} \text{degree}(v) & v = v' \\ -1 & \{v, v'\} \in E \\ 0 & \text{otherwise,} \end{cases} \quad (7.4)$$

which generalises (6.3), and  $F_\theta$ ,  $\theta = (\theta_1, \theta_2)$  is a lateral translation of  $\theta_1$  pixels south and  $\theta_2$  pixels east. per unit of time, i.e.

$$F_\theta(x) = \theta_1 \rho \nabla^\downarrow x + \theta_2 \rho \nabla^\leftarrow x,$$

where  $\nabla^\downarrow = \nabla^{(0, -1)}$  and  $\nabla^\leftarrow = \nabla^{(-1, 0)}$  are given by the mass transport operators

$$\nabla_{v,v'}^{(\Delta i, \Delta j)} = \begin{cases} -1 & v = v' \\ 1 & v = (i, j), v' = (i + \Delta i, j + \Delta j) \\ 0 & \text{otherwise} \end{cases}$$

with  $(\Delta i, \Delta j) \in \{(-1, 0), (1, 0), (0, 1), (0, -1)\}$ . Thus  $b_\theta(t, x) = -\frac{\sigma^2}{2}(\rho\Lambda + cI)x + F_\theta(x)$  with  $\theta$  considered as unknown parameter is of the form prescribed by Proposition 5.6. Choosing  $\rho$  and  $\sigma$  proportional to image scale makes the model roughly scale invariant, which informally can be seen from considering the stationary distribution given by the Lyapunov equation under transformation of the SDE by a linear downsampling operator  $R: \mathbb{R}^{m \times n} \rightarrow \mathbb{R}^{m/2 \times n/2}$ , assuming  $n, m$  are even. We then chose parameters which worked well at  $20 \times 24$  pixel resolution and scaled them to other resolutions  $41 \times 49$  and  $55 \times 65$  that we use. While the model works for finite dimensional problem at hand, the spatial white observation noise has no infinite dimensional scaling limit and for larger applications one would consider smoother observation noise with spatial correlation given by a non-diagonal covariance structure.



FIGURE 7. In the *pdf* version: The center panel shows the posterior mean trajectory  $x^*$  as animation. The left frame shows the first observation and the right frame shows the last of the four observations in the same resolution, showing that the latent convective system bridge moves smoothly from initial to the final state. The animation is also available as supplementary file.

**Parameter choices:** We set a scale  $\rho = 8m/195$  (which amounts to  $8/3$  for the highest resolution level) and take  $c = 0.1\rho$ . We set  $\sigma = 0.08\rho$ . The noise level is set to  $\sigma_\epsilon = 0.05\sqrt{\rho}$ . We took the time step as  $\delta t = 1/(35\rho)$ . We assume that  $X_T$  is a priori Gaussian with mean 0.5 (a grey value) and variance  $2.5I$  and equip  $\theta$  with an improper uniform prior.

**Algorithm details:** The SDE in our model is linear, so with  $\tilde{X} = X$ , the proposal is a sample from the conditional distribution and no change of measure is needed. We solve the backward filtering equations from Theorem 3.4 for  $\nu$  and  $P$  using the Euler scheme in combination with the enforced sparsity method from Subsection 6.2 using Julia’s native sparse matrix type (CSC). We took  $\varepsilon = 10^{-8}$ .

We employed Rao-Blackwellisation to obtain an estimate of the mean of the joint posterior of parameters and latent path, where in one step, the mean of  $X^*$  given observations and  $\theta$  is given by

$$dx_t^* = b_\theta(t, x_t^*) dt + \sigma^2 P(t)^{-1} (x_t^* - \nu(t)) dt, \quad x_0^* = \nu(0)$$

and in the second step the mean of  $\theta$  given  $X^*$  is obtained using Proposition 5.6.

For the correction formulas (3.15) we opted for an implementation based on the sparse Cholesky factorisation provided in Julia.

**Results:** The first 15 steps of the algorithm were run on a model down-scaled to lower resolution, for the subsequent 15 steps the resolution was increased and the final 15 steps were run on a model with the chosen, target resolution. Figure 8 shows the trace of  $\theta_1$ , and  $\theta_2$  for 45 iterates of the Rao-Blackwellised chain. After the last 15 steps the final estimates of the posterior means of the parameters are obtained as  $\hat{\theta}_1 = 1.55$  and  $\hat{\theta}_2 = 6.12$ . These are in good agreement with visual assessment of the movement. The estimates of  $\theta$  appear mostly stable at different model scales. (See the small changes in the estimates after each change of resolution at steps 15 and 30 in Figure 8.) The animation in Figure 7 shows the estimated posterior mean trajectory. The incorporation of discrete time observations with continuous latent dynamics and a drift term allows the algorithm to recognise the convective system as one object even if it has moved a substantial amount of pixels.

We only report rough timings: backward filtering step took half a minute for the correction steps and about two minutes for propagating the uncertainty at full resolution. Forward guiding took about half a minute and the parameter update about 1 second. (Timings are variable and depend on the current value of  $\theta$ , as  $\theta$  influences the sparsity.) The Kalman gain had 3 % non-zero entries with  $\epsilon = 10^{-8}$ .

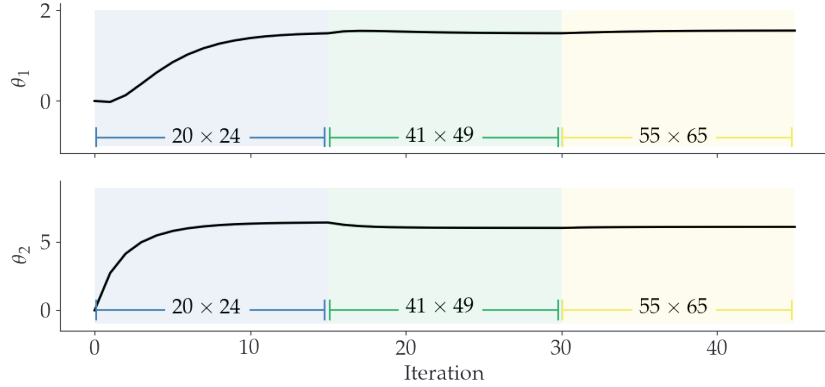


FIGURE 8. Iterates of  $\theta_1, \theta_2$  starting in  $\theta_1 = \theta_2 = 0$  from Rao-Blackwellisation with increasing dimension. First 15 iterates (blue): running with resolution  $20 \times 24$ . Next 15 iterates (green): continuing with resolution  $41 \times 49$ . Last 15 iterates (yellow): full resolution  $55 \times 65$ .

### Appendix A: The precise meaning of the guiding term in $X^*$

Here we explain the precise type of conditioning induced by the guiding term in  $X^*$ . In particular, the specific form of  $\rho$  in (1.3).

It suffices to consider  $t \in [0, t_1)$  and future observations at times  $t_1 < t_2 < \dots < t_n$ . Let  $y \in \mathbb{R}^d$ . Define  $\xi = (\xi_1, \dots, \xi_n)$  and  $\mathbf{v} = (v_1, \dots, v_n)$ . Consider the statistical model where the parameter is  $\xi$  and observation vector  $\mathbf{v}$  satisfies

$$v_j - L_j \xi_j \stackrel{\text{ind}}{\sim} q_j, \quad 1 \leq j \leq n. \quad (\text{A.1})$$

We will assume  $\xi_j \in \mathbb{R}^d$ ,  $L_j \in \mathbb{R}^{m_j \times d}$  and  $v_j \in \mathbb{R}^{m_j}$ . Then the likelihood for  $\xi$  based on observations  $\mathbf{v}$  is given by

$$L(\xi \mid \mathbf{v}) = \prod_{j=1}^n q_j(v_j - L_j \xi_j).$$

For a fixed pair  $(t, y)$ , define a prior distribution on  $\xi$  by

$$\pi_{(t,y)}(\xi) = p(t, y; t_1, \xi_1) \prod_{j=1}^n p(t_j, \xi_j; t_{j+1}, \xi_{j+1}). \quad (\text{A.2})$$

Starting from the diffusion process  $X$  (with the drift and diffusion coefficients  $b$  and  $\sigma$  respectively) satisfying  $X_0 = x_0$ , we apply Doob's  $h$ -transform with

$$h(t, y) = \frac{\int \pi_{(t,y)}(\xi) L(\xi \mid \mathbf{v}) d\xi}{\int \pi_{(0,x_0)}(\xi) L(\xi \mid \mathbf{v}) d\xi}.$$

Suppose  $X$  has measure  $\mathbb{P}$  on  $C([0, t_n], \mathbb{R}^d)$  and set  $Z_t = h(t, X_t)$ . It is easily verified that for any  $t < t_1$ ,  $Z_t$  is a martingale with mean 1. Define a new probability measure  $\mathbb{Q}$  on the same filtered measure space on which  $P$  is defined, via the relation  $d\mathbb{Q}|_{\mathcal{F}_t} = Z_t d\mathbb{P}|_{\mathcal{F}_t}$ ,  $\forall t \in [0, t_1]$ . By Girsanov's theorem it follows that under  $\mathbb{Q}$

$$dX_t = b(t, X_t) dt + \sigma(t, X_t) d\tilde{W}_t + a(t, X_t)' \nabla \log h(t, X_t) dt,$$

where  $\tilde{W}$  is Brownian motion under  $\mathbb{Q}$ . We have

$$\begin{aligned}\mathbb{E}_{\mathbb{Q}} f(X_t) &= \mathbb{E}_{\mathbb{P}}[Z_t f(X_t)] = \mathbb{E}_{\mathbb{P}}[h(t, X_t) f(X_t)] = \int f(y) p(0, x_0; t, y) h(t, y) dy \\ &= \int f(y) p(0, x_0; t, y) \frac{\pi_{(t,y)}(\xi) L(\xi | v) d\xi}{\pi_{(0,x_0)}(\xi) L(\xi | v) d\xi} dy \\ &= \int \left( \int f(y) \frac{p(0, x_0; t, y) \pi_{(t,y)}(\xi)}{\pi_{(0,x_0)}(\xi)} dy \right) \psi(\xi) d\xi\end{aligned}$$

where we used Fubini as the final equality and  $\psi$  is defined by

$$\psi(\xi) = \frac{\pi_{(0,x_0)}(\xi) L(\xi | v)}{\int \pi_{(0,x_0)}(\xi) L(\xi | v) d\xi}.$$

Therefore, we have

$$\mathbb{E}_{\mathbb{Q}} f(X_t) = \int \mathbb{E}_{\mathbb{P}}[f(X_t) | X_{t_1} = \xi_1, \dots, X_{t_n} = \xi_n] \psi(\xi) d\xi.$$

This shows that under  $\mathbb{Q}$ , first  $\xi$  is sampled from the density  $\psi$ , and subsequently the process  $X$  is conditioned on the event  $\{X_{t_1} = \xi_1, \dots, X_{t_n} = \xi_n\}$ . Now sampling from  $\psi$  corresponds to sampling from the posterior of  $\xi$  in the statistical model specified by (A.1) with prior specified by (A.2).

## Appendix B: Proofs of theorems in Section 3 and additional remarks

In the proofs we will assume observation times  $0 < S < T$  and observations  $V_S \sim \mathcal{N}(L_S X_S, \Sigma_S)$  and  $V_T \sim \mathcal{N}(L_T X_T, \Sigma_T)$  with  $L_S \in \mathbb{R}^{m_S \times d}$  and  $L_T \in \mathbb{R}^{m_T \times d}$ ; the extension to multiple future conditionings being trivial.

### B.1. Proof of Theorem 3.2

Define  $\Phi$  to be the solution to  $d\Phi(t) = B(t)\Phi(t) dt$  with  $\Phi(0) = I$ . Set  $\Phi(t, s) = \Phi(t)\Phi(s)^{-1}$ . Define

$$\Upsilon(t) = \begin{cases} \begin{bmatrix} \Sigma_S & 0_{m_S \times m_T} \\ 0_{m_T \times m_S} & \Sigma_T \end{bmatrix} & t \in (0, S] \\ \Sigma_T & t \in (S, T] \end{cases},$$

and notice (upon differentiation) that

$$L(t) = \begin{cases} \begin{bmatrix} L_S \Phi(S, t) \mathbf{1}_{(0,S]}(t) \\ L_T \Phi(T, t) \end{bmatrix} & t \in (0, S] \\ L_T \Phi(T, t) & t \in (S, T] \end{cases}, \quad (\text{B.1})$$

$$M^\dagger(t) = \int_t^T L(\tau) \tilde{a}(\tau) L(\tau)' d\tau + \Upsilon(t), \quad (\text{B.2})$$

and

$$\mu(t) = \int_t^T L(\tau) \beta(\tau) d\tau, \quad t \in [0, T], \quad (\text{B.3})$$

are the solutions to ODEs (3.1), (3.2) and (3.3) respectively. Note that  $\mu(t) \in \mathbb{R}^{m(t)}$  and that  $\Upsilon(t)$ ,  $L(t)$ ,  $M^\dagger(t)$  and  $v(t)$  have similar structures when  $t$  is either in  $(0, S]$  or  $(S, T]$ . The relations in (3.4) can be verified by evaluating  $L(t)$  for both  $t = S$  and  $t = S+$  (and similarly for  $M^\dagger(t)$  and  $\mu(t)$ ).

As we assume  $\Sigma_T$  to be strictly positive definite, matrix  $M(t) = M^\dagger(t)^{-1}$  exists for  $t \in [0, T]$  (see however Remark B.2 in case of no noise on the observations).

The expression for  $\tilde{r}$  for  $t \in (0, S]$  follows by extending Lemma 2.5 in [van der Meulen and Schauer \(2017b\)](#) to the case where not necessarily  $\Sigma_T = 0$  and  $L_T = I$ . The expressions for  $t \in (S, T]$  follow from equation (4.1) in [van der Meulen and Schauer \(2017b\)](#).

To derive  $\tilde{\rho}$ , note by [Schauer et al. \(2017, Section 5\)](#) that  $\tilde{X}$  is a Gaussian process with conditional mean  $\mu_t(s, x) = \mathbb{E}[\tilde{X}_t | \tilde{X}_s = x]$  and covariance  $K_t(s) = \text{Cov}(\tilde{X}_s, \tilde{X}_t)$ , where:

$$\mu_t(s, x) = \Phi(t, s)x + \int_s^t \Phi(s, \tau)\beta(\tau) d\tau, \quad K_t(s) = \int_s^t \Phi(t, \tau)\tilde{a}(\tau)\Phi(t, \tau)' d\tau. \quad (\text{B.4})$$

Then, clearly,  $(V'_S, V'_T)' = ((L_S \tilde{X}_S + \eta_S)', (L_T \tilde{X}_T + \eta_T)')'$  is Gaussian as well and its mean (denoted with  $\bar{v}(t)$ ) and covariance (denoted with  $\bar{\Omega}(t)$ ) are given by:

$$\bar{v}(t) = \begin{pmatrix} L_S \mu_S(t, x) \\ L_T \mu_T(t, x) \end{pmatrix}, \quad \bar{\Omega}(t) = \begin{pmatrix} L_S K_{SS} L'_S + \Sigma_S & L_S K_{ST} L'_T \\ L_T K_{TS} L'_S & L_T K_{TT} L'_T + \Sigma_T \end{pmatrix},$$

where  $K_{\tau\nu} = K_{\tau\wedge\nu}(t)$ ,  $\tau, \nu \in [t, T]$ . Careful comparison of  $\bar{v}(t)$  and  $\bar{\Omega}(t)$  with the definitions (B.1), (B.2) and (B.3) reveals that

$$\bar{v}(t) = L(t)x + \mu(t), \quad \bar{\Omega}(t) = M^\dagger(t),$$

and the expression for  $\tilde{\rho}$  follows.

**Remark B.1.** The value of Theorem 3.2 lies in recognition of the structure on both  $H$  and  $\tilde{r}$ , something which was not noticed in [van der Meulen and Schauer \(2017b\)](#). The theorem shows that both quantities can be written in a unified way on both  $(0, S]$  and  $(S, T]$ . The key to this is the proper definition of  $L$  (including the indicator).

**Remark B.2.** Suppose  $L_T = I$  and  $\Sigma_T \equiv 0$ . For  $t \in (S, T]$ ,  $M(t)$  exists if and only if  $\int_t^T \Phi(T, \tau)\tilde{a}(\tau)\Phi(T, \tau)' d\tau$  is invertible. This matrix is the controllability Gramian. Systems theory provides sufficient conditions for controllability. In case  $\tilde{a}(t)$  is not invertible, then  $M(t)$  exists if and only if the pair of functions  $(B, \tilde{\sigma})$  is controllable on  $[t, T]$  for any  $t \in [0, T]$  (cf. Section 5.6 in [Karatzas and Shreve \(1991\)](#)).

**Remark B.3.** Suppose  $L_S = I$  and  $\Sigma_S = 0$ . This corresponds to the case where the diffusion is fully observed at time  $S$  without noise. By the Markov property, the pulling term should only depend on  $v_S$  (which is then in fact  $x_S$ ) and not on  $v_T$ . To verify this, first note that we can write

$$M^\dagger(t) = \begin{bmatrix} A & C \\ C' & D \end{bmatrix},$$

where for  $t \in [0, S]$

$$\begin{aligned} A &= \int_t^S L_S \Phi(S, \tau) \tilde{a}(\tau) \Phi(S, \tau)' d\tau, \\ C &= \int_t^S L_S \Phi(S, \tau) \tilde{a}(\tau) \Phi(T, \tau)' L_T' d\tau = A \Phi(T, S)' L_T', \\ D &= \int_t^T L_T \Phi(T, \tau) \tilde{a}(\tau) \Phi(T, \tau)' L_T' d\tau. \end{aligned}$$

Now assume  $L_S = I$  and that  $A$  is invertible. Then we have

$$L(t) = \begin{bmatrix} L_S \\ L_T \Phi(T, S) \end{bmatrix} \Phi(S, t) = \begin{bmatrix} I \\ C' A^{-1} \end{bmatrix} \Phi(S, t).$$

Let  $Z = (D - C' A^{-1} C)^{-1}$ . Using the formula for the inverse of a block matrix, we get

$$\begin{aligned} H(t) &= \Phi(S, t)' \begin{bmatrix} I & A^{-1} C \end{bmatrix} \begin{bmatrix} A^{-1} + A^{-1} C Z C' A^{-1} & -A^{-1} C Z \\ -Z C' A^{-1} & Z \end{bmatrix} \begin{bmatrix} I \\ C' A^{-1} \end{bmatrix} \Phi(S, t) \\ &= \Phi(S, t)' A^{-1} \Phi(S, t) = \left( \int_t^S \Phi(t, \tau) \tilde{a}(\tau) \Phi(t, \tau)' d\tau \right)^{-1}. \end{aligned}$$

This is exactly as in Lemma 6 of [Schauer et al. \(2017\)](#).

**Remark B.4.** Suppose  $t \in (t_{i-1}, t_i]$  and we condition on future incomplete observations  $(v_i, \dots, v_n)$ . In that setting the correct definitions for  $\Upsilon$  and  $L(t)$  are

$$\Upsilon(t) = \text{diag}(\Sigma_i, \dots, \Sigma_n) \quad \text{and} \quad L(t) = \begin{bmatrix} L_i \Phi(t_i, t) \\ L_{i+1} \Phi(t_{i+1}, t) \\ \dots \\ L_n \Phi(t_n, t) \end{bmatrix}$$

## B.2. Proof of Theorem 3.3

The expression for  $\log \tilde{\rho}$  follows from Theorem 3.2 by simple algebra, with

$$\begin{aligned} c(t) &= \frac{1}{2} C_t^{(1)} + C_t^{(2)}, \quad \text{where} \\ C_t^{(1)} &= (v(t) - \mu(t))' M(t) (v(t) - \mu(t)) \quad \text{and} \quad C_t^{(2)} = \log \left[ (2\pi)^{m(t)/2} |M^\dagger(t)|^{1/2} \right]. \end{aligned} \tag{B.5}$$

**Backward ordinary differential equations** We derive the ordinary differential equations solved by  $H(t)$ ,  $F(t)$  and  $c(t)$  in a neighbourhood disjoint from  $\{S, T\}$ . We start with  $H(t)$ .

$$\begin{aligned} \frac{d}{dt} H(t) &= \left( \frac{d}{dt} L(t) \right)' M(t) L(t) + L(t)' \left( \frac{d}{dt} M(t) \right) L(t) + L(t)' M(t) \left( \frac{d}{dt} L(t) \right) \\ &= -B(t)' L(t)' M(t) L(t) + L(t)' \left( \frac{d}{dt} M(t) \right) L(t) - L(t)' M(t) L(t) B(t) \\ &\quad - B(t)' H(t) - H(t) B(t) + L(t)' \left( \frac{d}{dt} M(t) \right) L(t). \end{aligned} \tag{B.6}$$

Since  $M(t) = (M^\dagger(t))^{-1}$ :

$$\frac{d}{dt}M(t) = -M(t) \left( \frac{d}{dt}M^\dagger(t) \right) M(t) = M(t)L(t)\tilde{a}(t)L(t)'M(t), \quad (\text{B.7})$$

and thus:

$$L(t)' \left( \frac{d}{dt}M(t) \right) L(t) = H(t)\tilde{a}(t)H(t).$$

Substituting this back into (B.6) yields:

$$dH(t) = (-B(t)'H(t) - H(t)B(t) + H(t)\tilde{a}(t)H(t)) dt.$$

For  $F(t)$  notice:

$$\begin{aligned} \frac{d}{dt}F(t) &= \left( \frac{d}{dt}L(t) \right)' M(t)(v(t) - \mu(t)) + L(t)' \left( \frac{d}{dt}M(t) \right) (v(t) - \mu(t)) \\ &\quad - L(t)'M(t) \left( \frac{d}{dt}\mu(t) \right) \\ &= -B(t)'L(t)'M(t)(v(t) - \mu(t)) \\ &\quad + L(t)'M(t)L(t)\tilde{a}(t)L(t)'M(t)(v(t) - \mu(t)) + L(t)'M(t)L(t)\beta(t) \\ &= -B(t)'F(t) + H(t)\tilde{a}(t)F(t) + H(t)\beta(t). \end{aligned}$$

For  $c(t)$  we differentiate  $C_t^{(1)}$  and  $C_t^{(2)}$  in turn. By (3.3), (B.7) and the definition of  $F(t)$ :

$$\begin{aligned} \frac{d}{dt}C_t^{(1)} &= -2 \left( \frac{d}{dt}\mu(t) \right)' M(t)(v(t) - \mu(t)) + (v(t) - \mu(t))' \left( \frac{d}{dt}M(t) \right) (v(t) - \mu(t)) \\ &= 2\beta(t)'L(t)'M(t)(v(t) - \mu(t)) + (v(t) - \mu(t))'M(t)L(t)\tilde{a}(t)L(t)'M(t)(v(t) - \mu(t)) \\ &= 2\beta(t)'F(t) + F(t)' \tilde{a}(t)F(t). \end{aligned} \quad (\text{B.8})$$

To find  $\frac{d}{dt}C_t^{(2)}$ , first, note by [Minka \(2000, eq. \(10\)\)](#) that for a matrix-valued function  $Y$ :

$$\frac{\partial|Y|}{\partial x} = |Y|\text{tr} \left( Y^{-1} \frac{\partial Y}{\partial x} \right),$$

which gives

$$\begin{aligned} \frac{d|M^\dagger(t)|}{dt} &= |M^\dagger(t)|\text{tr} \left( M(t) \frac{dM^\dagger(t)}{dt} \right) \\ &= |M^\dagger(t)|\text{tr}(-M(t)L(t)\tilde{a}(t)L(t)') \\ &= -|M^\dagger(t)|\text{tr}(L(t)'M(t)L(t)\tilde{a}(t)) = -|M^\dagger(t)|\text{tr}(H(t)\tilde{a}(t)). \end{aligned}$$

Since at non-observation times  $t$ ,  $m(t)$  is constant, the chain rule implies

$$\frac{d}{dt}C_t^{(2)} = -\frac{1}{2}\text{tr}(H(t)\tilde{a}(t)). \quad (\text{B.9})$$

Combining (B.8) and (B.9) yields the ODE for  $c(t)$  stated in Theorem 3.3.

**Update equations** The boundary conditions for  $H(T)$ ,  $F(T)$ ,  $C_T^{(1)}$  and  $C_T^{(2)}$ :

$$H(T) = L'_T \Sigma_T^{-1} L_T, \quad F(T) = L'_T \Sigma_T^{-1} v_T, \quad C_T^{(1)} = v_T \Sigma_T^{-1} v_T, \quad C_T^{(2)} = \frac{m_T}{2} \log(2\pi) + \frac{1}{2} \log |\Sigma_T|,$$

follow directly from the definitions:  $L(T) = L_T$ ,  $M(T) = \Sigma_T^{-1}$  and  $\mu(T) = 0$ ; as well as the expressions for  $H(t)$ ,  $F(t)$ ,  $C_t^{(1)}$  and  $C_t^{(2)}$  given in (3.5), (3.6) and (B.5) respectively. The boundary condition for  $c(T)$  follows immediately

$$c(T) = \frac{1}{2} C_T^{(1)} + C_T^{(2)} = \frac{1}{2} v_T \Sigma_T^{-1} v_T + \frac{m_T}{2} \log(2\pi) + \frac{1}{2} \log |\Sigma_T|.$$

Now, combining the expressions for  $H(t)$ ,  $F(t)$  and  $C_t^{(1)}$ , given in (3.5), (3.6) and (B.5) respectively, with the update equations for  $L(S)$ ,  $M(S)$  and  $\mu(S)$  at time  $S$ , given in Theorem 3.2, yields the update equations for  $H(S)$ ,  $F(S)$  and  $C_S^{(1)}$ :

$$H(S) = H(S+) + L'_S \Sigma_S^{-1} L_S, \quad F(S) = F(S+) + L'_S \Sigma_S^{-1} v_S, \quad C_S^{(1)} = C_{S+}^{(1)} + v_S \Sigma_S^{-1} v_S. \quad (\text{B.10})$$

To derive the update equations for  $C_S^{(2)}$ , notice that at observation time  $S$  we have

$$\begin{aligned} \tilde{\rho}(S, x) &= \varphi(v_S; L_S x, \Sigma_S) \tilde{\rho}(S+, x) \\ &= (2\pi)^{-m_S/2} |\Sigma_S|^{-1/2} \exp\left(-\frac{1}{2}(v_S - L_S x)' \Sigma_S^{-1} (v_S - L_S x)\right) \times \exp\left(-C_{S+}^{(2)}\right) \\ &\quad \times \exp\left(-\frac{1}{2}(v(S+) - \mu(S+) - L(S+)x)' M(S+) (v(S+) - \mu(S+) - L(S+)x)\right). \end{aligned}$$

This can be written as

$$\exp\left(-C_S^{(2)}\right) \exp\left(-\frac{1}{2}(v(S) - \mu(S) - L(S)x)' M(S) (v(S) - \mu(S) - L(S)x)\right),$$

upon defining

$$C_S^{(2)} = C_{S+}^{(2)} + \frac{m_S}{2} \log(2\pi) + \frac{1}{2} \log |\Sigma_S| \quad (\text{B.11})$$

and because we have

$$v(S) = \begin{bmatrix} v_S \\ v(S+) \end{bmatrix} \quad \mu(S) = \begin{bmatrix} 0 \\ \mu(S+) \end{bmatrix} \quad L(S) = \begin{bmatrix} L_S \\ L(S+) \end{bmatrix} \quad M(S) = \begin{bmatrix} \Sigma_S^{-1} & 0 \\ 0 & M(S+) \end{bmatrix}.$$

Cobining (B.10) and (B.11) yields the update equation for  $c(S)$

$$c(S) = \frac{1}{2} C_S^{(1)} + C_S^{(2)} = c(S+) + v_S \Sigma_S^{-1} v_S + \frac{m_S}{2} \log(2\pi) + \frac{1}{2} \log |\Sigma_S|.$$

### B.3. Proof of Theorem 3.4

We first give the derivation for the ODE of  $P(t)$ . The derivation of the differential equation is the same whether we consider  $t \in [0, S]$  or  $t \in (S, T]$ . In particular, the ODE for  $H$  from Theorem 3.3 and the definition of  $P$  imply that

$$\frac{dP(t)}{dt} = -P(t) \left( \frac{d}{dt} H(t) \right) P(t) = P(t) B(t)' + B(t) P(t) - \tilde{a}(t).$$

The update formula from time  $S+$  to  $S$  follows from the corresponding one in terms of  $H$  and applying Woodbury's formula.

The derivation of the differential equation for  $\nu$  is the same whether we consider  $t \in [0, S]$  or  $t \in (S, T]$ . We have, using (B.12), (B.7) and (3.1)

$$\frac{d}{dt} (P(t)L(t)'M(t)) = B(t)P(t)L(t)'M(t). \quad (\text{B.12})$$

Using (3.3) we get

$$\frac{d}{dt} (v(t) - \mu(t)) = L(t)\beta(t).$$

The previous two equations together yield

$$\begin{aligned} \frac{d}{dt} \nu(t) &= B(t)P(t)L(t)'M(t) (v(t) - \mu(t)) + P(t)L(t)'M(t)L(t)\beta(t) \\ &= B(t)\nu(t) + \beta(t). \end{aligned}$$

The value of  $\nu(T)$  follows from  $P(T) = (L_T'\Sigma_T^{-1}L_T)^{-1}$ ,  $L(T) = L_T$ ,  $M(T) = \Sigma_T^{-1}$ ,  $v(T) = v_T$  and  $\mu(T) = 0$ .

To obtain the expression for  $\nu(S)$ , note that

$$\begin{aligned} \nu(S) &= P(S)L_S'M(S)(v(S) - \mu(S)) \\ &= P(S) \begin{bmatrix} L_S \\ L(S+) \end{bmatrix} \begin{bmatrix} \Sigma_S & 0 \\ 0 & M(S+) \end{bmatrix}^{-1} \left( \begin{bmatrix} v_S \\ v(S+) \end{bmatrix} - \begin{bmatrix} 0 \\ \int_s^T L_T\Phi(T, \tau)\beta(\tau) d\tau \end{bmatrix} \right) \\ &= P(S) (L_S'\Sigma_S^{-1}v_S + L(S+)M(S+)(v(S+) - \mu(S+))) \\ &= P(S) (L_S'\Sigma_S^{-1}v_S + H(S+)\nu(S+)). \end{aligned}$$

*Proof of Proposition 3.5.*

$$\begin{aligned} \frac{d}{dt} P(t) &= \frac{d}{dt} (\Phi(t, T)(\Sigma + P(T))\Phi(t, T) - \Sigma) \\ &= \left( \frac{d}{dt} \Phi(t, T) \right) (\Sigma + P(T))\Phi(t, T) + \Phi(t, T)(\Sigma + P(T)) \frac{d}{dt} \Phi(t, T)' \\ &= B\Phi(t, T)(\Sigma + P(T))\Phi(t, T)' + \Phi(t, T)(\Sigma + P(T))\Phi(t, T)'B' \\ &= B(P(t) + \Sigma) + (P(t) + \Sigma)B' = BP(t) + P(t)B' - \tilde{a}, \end{aligned}$$

where we used (3.17) at the third equality and  $\Sigma$  solving the Lyapunov equation at the final equality.  $\square$

**Remark B.5.** We investigate the behaviour of  $P(S)$  and  $\nu(S)$  when the noise level tends to zero. Assume  $L_S P(S+) L_S'$  is invertible. Then it follows from (3.15) that the expression for  $P(S)$  is also well defined when  $\|\Sigma\| \rightarrow 0$ . Moreover, when  $\Sigma = 0$  we have

$$L_S P(S) = L_S P(S+) - L_S P(S+) L_S' (L_S P(S+) L_S')^{-1} L_S P(S+) = 0.$$

To evaluate the limiting behaviour of  $\nu(S)$ , we write

$$L_S \nu(S) = L_S P(S) L_S' \Sigma_S^{-1} v_S + L_S P(S) H(S+) \nu(S+).$$

The second term on the right-hand-side is easily seen to tend to zero when  $\|\Sigma_S\| \rightarrow 0$ . For deriving the limit of the first term on the right-hand-side we define  $C = L_S P(S+) L'_S \Sigma_S^{-1}$  and rewrite

$$\begin{aligned} L_S P(S) L'_S \Sigma_S^{-1} &= L_S P(S+) L'_S \Sigma_S^{-1} \\ &\quad - L_S P(S+) L'_S (\Sigma_S + L_S P(S+) L'_S \Sigma_S^{-1} \Sigma_S)^{-1} L_S P(S+) L'_S \Sigma_S^{-1} \\ &= C - C(I + C)^{-1} C = (I + C^{-1})^{-1}, \end{aligned}$$

where we used Woodbury's formula at the final equality. Now

$$C^{-1} = \Sigma_S (L_S P(S+) L'_S)^{-1} \rightarrow 0, \quad \text{when } \|\Sigma_S\| \rightarrow 0.$$

This implies that  $L_S P(S) L'_S \Sigma_S^{-1} \rightarrow I$ . Combining these results we obtain that

$$L_S \nu(S) \rightarrow v_S, \quad \text{when } \|\Sigma_S\| \rightarrow 0.$$

In particular, if we have full observations at time  $S$ , i.e.  $L_S = I$ , then  $P(S) \rightarrow 0$  and  $\nu(S) \rightarrow v_S$  if  $\|\Sigma_S\| \rightarrow 0$ . As a consequence, in case of full observations and no noise, we recover the full observation without noise case (in this simpler setting, the differential equations for  $\nu$  and  $P$  were derived in [van der Meulen and Schauer \(2017c\)](#)). However, in the general case where  $L_S$  is not of full rank, we need that  $\det \Sigma_S \neq 0$  to obtain the value of  $\nu(S)$  from  $\nu(S+)$ .

## Appendix C: Implementation using a time-change and scaling

If the noise level on the observation is small, care is required in the discretisation of guided proposals near the conditioning points. For this reason, a time-change and scaling was introduced in Section 5 of [van der Meulen and Schauer \(2017a\)](#). Here, we explain it for the case of 2 future conditionings. Define the mapping  $\tau : [0, S+T] \rightarrow [0, S+T]$  by

$$\tau(s) = \begin{cases} s(2 - \frac{s}{S}) & \text{if } s \in [0, S] \\ S + (s - S)\left(2 - \frac{s-S}{T-S}\right) & \text{if } s \in [S, T] \end{cases}.$$

For a mapping  $f : \mathbb{R} \rightarrow \mathbb{R}$  we write  $f_\tau(s) = f(\tau(s))$ . We propose to discretise the process  $U_s$ , defined by

$$U_s = \frac{\nu_\tau(s) - X_{\tau(s)}^\circ}{\dot{\tau}(s)},$$

instead on  $X_s^\circ$ . This process satisfies the SDE

$$\begin{aligned} dU_s &= (B_\tau(s)v_\tau(s) + \beta_\tau(s) - b_\tau(s, U_s)) ds \\ &\quad - \left( \frac{\ddot{\tau}(s)}{\dot{\tau}(s)} I + a_\tau(s, U_s) J(s) \right) U_s ds \\ &\quad + \frac{1}{\sqrt{\dot{\tau}(s)}} \sigma_\tau(s, U_s) dW_s, \quad U_0 = \frac{\nu_\tau(0) - x_0}{2} \end{aligned}$$

Here,  $J$  is defined by

$$J(s) = \dot{\tau}(s) H_\tau(s).$$

Furthermore, we have used the notation  $b_\tau(s, y) = b(\tau(s), v_\tau(s) - \dot{\tau}(s)y)$  and similarly for  $\sigma_\tau$  and  $a_\tau$ . For the likelihood ratio (2.3), note that  $\tilde{r}(\tau(s), X_{\tau(s)}^\circ) = J(s)U_s$ .

$$\begin{aligned} \int_0^T G(s, X_s^\circ) ds &= \int_0^T (b_\tau(s, U_s) - B_\tau(s, U_s)) J(s)U_s \dot{\tau}(s) ds \\ &\quad - \frac{1}{2} \int_0^T \text{tr} (\{a_\tau(s, U_s) - \tilde{a}_\tau(s)\} \{J(s) - J(s)U_s U_s' J(s) \dot{\tau}(s)\}) ds \end{aligned}$$

Finally, by the chain-rule,  $P_\tau(s)$  and  $\nu_\tau(s)$  satisfy the backward differential equations

$$\frac{d}{dt} P_\tau(t) = (B_\tau(t)P_\tau(t) + P_\tau B_\tau(t)' - \tilde{a}_\tau(t)) \dot{\tau}(s)$$

and

$$\frac{d}{dt} \nu_\tau(t) = (B_\tau(t)\nu_\tau(t) + \beta_\tau(t)) \dot{\tau}(s).$$

## Acknowledgments

The research leading to the results in this paper has received funding from the European Research Council under ERC Grant Agreement 320637. M.M. was sponsored by the Max Planck Institute for Mathematics in the Sciences, Leipzig and the EPSRC [grant number EP/L016710/1].

## References

Apte, A., Hairer, M., Stuart, A. and Voss, J. (2007). Sampling the posterior: An approach to non-gaussian data assimilation. *Physica D: Nonlinear Phenomena* **230**(1), 50 – 64. Data Assimilation.

Arkin, A., Ross, J. and McAdams, H. H. (1998). Stochastic kinetic analysis of developmental pathway bifurcation in phage  $\lambda$ -infected Escherichia coli cells. *Genetics* **149**(4), 1633–1648.

Arnaudon, A., Holm, D. D. and Sommer, S. (2017). A geometric framework for stochastic shape analysis. *ArXiv e-prints* **1703.09971**.

Arnaudon, A., van der Meulen, F., Schauer, M. and Sommer, S. (2020). Diffusion bridges for stochastic hamiltonian systems with applications to shape analysis.

Avenel, C., Mémin, E. and Pérez, P. (2014). Stochastic level set dynamics to track closed curves through image data. *Journal of Mathematical Imaging and Vision* **49**(2), 296–316.

Bayer, C. and Schoenmakers, J. (2013). Simulation of forward-reverse stochastic representations for conditional diffusions. *Ann. Appl. Probab.* To appear.

Beskos, A., Papaspiliopoulos, O., Roberts, G. O. and Fearnhead, P. (2006). Exact and computationally efficient likelihood-based estimation for discretely observed diffusion processes. *J. R. Stat. Soc. Ser. B Stat. Methodol.* **68**(3), 333–382. With discussions and a reply by the authors.

Beskos, A., Roberts, G., Stuart, A. and Voss, J. (2008). Mcmc methods for diffusion bridges. *Stochastics and Dynamics* **08**(03), 319–350.

Beskos, A. and Roberts, G. O. (2005). Exact simulation of diffusions. *Ann. Appl. Probab.* **15**(4), 2422–2444.

Bezanson, J., Edelman, A., Karpinski, S. and Shah, V. B. (2017). Julia: a fresh approach to numerical computing. *SIAM Rev.* **59**(1), 65–98.

Bierkens, J., van der Meulen, F. and Schauer, M. (2019). Simulation of elliptic and hypo-elliptic conditional diffusions. *Accepted for publication in Advances in Applied Probability*.

Bladt, M., Finch, S. and Sørensen, M. (2016). Simulation of multivariate diffusion bridges. *J. R. Stat. Soc. Ser. B. Stat. Methodol.* **78**(2), 343–369.

Clark, J. M. C. (1990). The simulation of pinned diffusions. In *Decision and Control, 1990., Proceedings of the 29th IEEE Conference on*, pp. 1418–1420. IEEE.

Cotter, S. L., Roberts, G. O., Stuart, A. M. and White, D. (2013). Mcmc methods for functions: Modifying old algorithms to make them faster. *Statist. Sci.* **28**(3), 424–446.

Cuenod, C.-A., Favetto, B., Genon-Catalot, V., Rozenholc, Y. and Samson, A. (2011). Parameter estimation and change-point detection from dynamic contrast enhanced {MRI} data using stochastic differential equations. *Mathematical Biosciences* **233**(1), 68 – 76.

Da Prato, G. and Zabczyk, J. (2014). *Stochastic Equations in Infinite Dimensions*. Encyclopedia of Mathematics and its Applications. Cambridge University Press, 2 edition.

Delyon, B. and Hu, Y. (2006). Simulation of conditioned diffusion and application to parameter estimation. *Stochastic Processes and their Applications* **116**(11), 1660 – 1675.

Durham, G. B. and Gallant, A. R. (2002). Numerical techniques for maximum likelihood estimation of continuous-time diffusion processes. *J. Bus. Econom. Statist.* **20**(3), 297–338. With comments and a reply by the authors.

Elerian, O., Chib, S. and Shephard, N. (2001). Likelihood inference for discretely observed nonlinear diffusions. *Econometrica* **69**(4), 959–993.

Eraker, B. (2001). MCMC analysis of diffusion models with application to finance. *J. Bus. Econom. Statist.* **19**(2), 177–191.

Evensen, G. (2003). The ensemble kalman filter: theoretical formulation and practical implementation. *Ocean Dynamics* **53**(4), 343–367.

Fearnhead, P., Papaspiliopoulos, O. and Roberts, G. O. (2008). Particle filters for partially observed diffusions. *J. R. Stat. Soc. Ser. B Stat. Methodol.* **70**(4), 755–777.

Fuchs, C. (2013). *Inference for diffusion processes*. Springer, Heidelberg. With applications in life sciences, With a foreword by Ludwig Fahrmeir.

Golightly, A. and Wilkinson, D. J. (2005). Bayesian inference for stochastic kinetic models using a diffusion approximation. *Biometrics* **61**(3), 781–788.

Golightly, A. and Wilkinson, D. J. (2008). Bayesian inference for nonlinear multivariate diffusion models observed with error. *Comput. Statist. Data Anal.* **52**(3), 1674–1693.

Golightly, A. and Wilkinson, D. J. (2011). Bayesian parameter inference for stochastic biochemical network models using particle Markov chain Monte Carlo. *Interface focus* **1**(6), 807–820.

Graham, M. M., Thiery, A. H. and Beskos, A. (2019). Manifold markov chain monte carlo methods for bayesian inference in a wide class of diffusion models.

Haario, H., Saksman, E., Tamminen, J. et al. (2001). An adaptive Metropolis algorithm. *Bernoulli* **7**(2), 223–242.

Hairer, M., Stuart, A. M. and Voss, J. (2009). Sampling conditioned diffusions. In *Trends in Stochastic Analysis*, volume 353 of *London Mathematical Society Lecture Note Series*, pp. 159–186. Cambridge University Press.

Hartog, J. and van Zanten, H. (2019). Nonparametric bayesian label prediction on a large graph using truncated laplacian regularization. *Communications in Statistics - Simulation and Computation* **0**(0), 1–18.

Houtekamer, P. L. and Mitchell, H. L. (2001). A sequential ensemble kalman filter for atmospheric data assimilation. *Monthly Weather Review* **129**(1), 123–137.

Karatzas, I. and Shreve, S. E. (1991). *Brownian motion and stochastic calculus*, volume 113 of *Graduate Texts in Mathematics*. Springer-Verlag, New York, second edition.

Kloeden, P. E. and Platen, E. (2013). *Numerical Solution of Stochastic Differential Equations*, volume 23. Springer Science & Business Media.

Lin, M., Chen, R. and Mykland, P. (2010). On generating Monte Carlo samples of continuous diffusion bridges. *J. Amer. Statist. Assoc.* **105**(490), 820–838.

Lindström, E. (2012). A regularized bridge sampler for sparsely sampled diffusions. *Stat. Comput.* **22**(2), 615–623.

Marchand, J.-L. (2012). *Conditionnement de processus markoviens*. IRMAR, Ph.d. Thesis Université de Rennes 1.

Mider, M., Schauer, M. and Grazzi, S. (2019). Bridgesdeinference v0.2.0. *Zenodo* (10.5281/zenodo.3525435).

Minka, T. P. (2000). Old and new matrix algebra useful for statistics. *Notes* .

Olsson, J. and Ströjby, J. (2011). Particle-based likelihood inference in partially observed diffusion processes using generalised Poisson estimators. *Electron. J. Stat.* **5**, 1090–1122.

Roberts, G. O. and Rosenthal, J. S. (2009). Examples of adaptive MCMC. *Journal of Computational and Graphical Statistics* **18**(2), 349–367.

Roberts, G. O. and Stramer, O. (2001). On inference for partially observed nonlinear diffusion models using the Metropolis-Hastings algorithm. *Biometrika* **88**(3), 603–621.

Särkkä, S. (2013). *Bayesian Filtering and Smoothing*. Cambridge University Press, New York, NY, USA.

Särkkä, S. and Sarmavuori, J. (2013). Gaussian filtering and smoothing for continuous-discrete dynamic systems. *Signal Processing* **93**(2), 500 – 510.

Särkkä, S. and Sottinen, T. (2008). Application of Girsanov theorem to particle filtering of discretely observed continuous-time non-linear systems. *Bayesian Anal.* **3**(3), 555–584.

Schauer, M. and contributors (2017). Bridge 0.7. *Zenodo* (10.5281/zenodo.1100978).

Schauer, M., van der Meulen, F. and van Zanten, H. (2017). Guided proposals for simulating multi-dimensional diffusion bridges. *Bernoulli* **23**(4A), 2917–2950.

Shephard, N. and Pitt, M. K. (1997). Likelihood analysis of non-Gaussian measurement time series. *Biometrika* **84**(3), 653–667.

van der Meulen, F. and Schauer, M. (2017a). Bayesian estimation of discretely observed multi-dimensional diffusion processes using guided proposals. *Electron. J. Stat.* **11**(1), 2358–2396.

van der Meulen, F. and Schauer, M. (2017b). Bayesian estimation of incompletely observed diffusions. *Stochastics* **0**(0), 1–22.

van der Meulen, F. and Schauer, M. (2017c). On residual and guided proposals for diffusion bridge simulation. *arXiv:1708.04870* .

Van der Meulen, F. H., Schauer, M. and Van Zanten, J. H. (2014). Reversible jump MCMC for nonparametric drift estimation for diffusion processes. *Comput. Statist. Data Anal.* **71**, 615–632.

van Kampen, N. G. (1981). *Stochastic processes in physics and chemistry*, volume 888 of *Lecture Notes in Mathematics*. North-Holland Publishing Co., Amsterdam-New York.

Verner, J. H. (1978). Explicit Runge–Kutta methods with estimates of the local truncation error. *SIAM Journal on Numerical Analysis* **15**(4), 772–790.

Whitaker, G. A., Golightly, A., Boys, R. J. and Sherlock, C. (2017). Improved bridge constructs for stochastic differential equations. *Statistics and Computing* **27**(4), 885–900.

Wilkinson, D. J. (2006). *Stochastic modelling for systems biology*. Chapman & Hall/CRC

Mathematical and Computational Biology Series. Chapman & Hall/CRC, Boca Raton, FL.